Real-time contextual feedback for close-loop control of navigation

Judith Lim and Tansu Celikel

Department of Neurophysiology, Donders Institute for Brain, Cognition, and Behaviour

Radboud University - the Netherlands

Correspondence should be addressed to j.lim@neurophysiology.nl and t.celikel@neurophysiology.nl

Abstract

Objective: Close-loop control of brain and behavior will benefit from real-time detection of behavioral events to enable low-latency communication with peripheral devices. In animal experiments, this is typically achieved by using sparsely distributed (embedded) sensors that detect animal presence in select regions of interest. High-speed cameras provide high-density sampling across large arenas, capturing the richness of animal behavior, however the image processing bottleneck prohibits real-time feedback in the context of rapidly evolving behaviors.

Approach: Here we developed an open-source software, named PolyTouch, to continuously track animal behavior in large arenas and provide rapid close-loop feedback in ~1ms, ie. flight-time including (auditory) stimulus delivery. This stand-alone, cross-platform software is written in JAVA. The included wrapper for MATLAB provides experimental flexibility for data acquisition, analysis and visualization.

Main results: As a proof-of-principle application we deployed the PolyTouch for place awareness training. A user defined portion of the arena was used as a virtual target; visit (or approach) to the target triggered auditory feedback. We show that mice develop awareness to virtual spaces, tend to stay shorter and move faster when they reside in the virtual target zone, if their visits are coupled to relatively high stimulus intensity (≥49dB). Thus, close-loop presentation of perceived aversive feedback is sufficient to condition mice to avoid virtual targets within the span of a single session (~20min).

Significance: Neuromodulation techniques now allow control of neural activity in a cell-type specific manner in spiking resolution. Using animal behavior to drive close-loop control of neural activity would help to address the neural basis of behavioral state and environmental context dependent information processing in the brain. Because PolyTouch enables neural feedback faster than sensory signals from the periphery take to reach central circuits, it could also be used to control sensory representations in real-time.

1. Introduction

Animal navigation is a product of close-loop neural computations. The brain computes a motor plan based on not only the sensory information it gathers from the world but also its expectations given the animal's previous experience and task-relevant requirements. For instance, a mouse navigating through a maze will alter its trajectory given its experience during prior exposures to the same arena [1–4], as motor strategies driving navigation are continuously shaped by external and internal signals [5–7]. Traditionally this close-loop control process is studied as an "open-loop" using a stimulus-response design, where a stimulus with a fixed temporal pattern evokes a behavioral or neural response that is typically analyzed offline. This provides only a correlative understanding of the inherent close-loop neural computations that underlie behavior. Instead, to causally address the neural circuits that give rise to dynamic behaviors, e.g. navigation, one needs to interfere with neural activity in the context of ongoing behavior.

Recent technological advancements have enabled researchers to close the loop [8,9] with real-time experimental control of neural [10–13] and behavioral signals [14–18]. In particular, close-loop optogenetic neural control has provided insight into cell-type-specific neuronal population dynamics in relation with seizure control [13,19,20], sensory perception [21], and spatial navigation [22]. Nevertheless, the real-time monitoring of behavior remains a challenging task for many researchers, because it demands (1) reliable event-detection at a high temporal resolution in real-time, (2) low-latency communication with peripheral devices to trigger feedback and (3) flexibility in terms of software and hardware integration. Previous animal studies have commonly used a single or array of infrared (IR) beam sensors to detect simple motion events (e.g. entering an area, lick in a reward port, [23] or a grid of sensors, including pressure sensors [24], to monitor locomotion with a delay in the millisecond range [1,2,4,25–27]) to overcome most of these limitations. Although these systems are fast and reliable, their spatial resolution is heavily limited by the number of sensors deployed. Despite the availability of various other sensors, including microwave based motion detectors [28], ultrasonic microphones [29,30], radiofrequency detectors [31], global positioning systems [32], and heat (infrared) sensors [33], majority of existing tracking systems rely on video cameras, as they provide detailed images of whole bodies [3,34–37],[38], individual limbs [39–41], face and whisker motion [42], and eye movements [43,44]. A major drawback, however, is that behavioral classification requires several image processing steps to detect and identify the object of interest which takes several tens of milliseconds using the current state-of-art algorithms and standard computing infrastructure. This typically prevents rapid, i.e. in the range of milliseconds, close-loop feedback. As an alternative, other studies have employed a hybrid touch-based imaging approach to counter the speed bottleneck of image processing pipelines [45–47]. In this approach, animal motion is tracked on a transparent surface, where contact points cause scattering of IR light that are captured with a camera. This produces high-contrast images and requires few image processing steps, and thus enables faster image processing.

The utility of touch-based methods in prior studies has not yet been generally extended to multi-touch interfaces [48],[49], in particular for rapid close-loop feedback applications. Since the introduction of accessible multi-

touch sensing technology in 2005 [50], most applications targeted human-computer interactions, including with mobile phones, tablets and virtual reality systems [51]. For this very reason, all modern computers and mobile computing devices come with built-in controller drivers for touch sensors that automatically recognize touch input. We extended the utility of this multi-touch technology to develop PolyTouch, an open-source software to track animal behavior in the open field using an IR sensor frame for real-time (delay: 1ms) close-loop feedback. The tracking software is multi-touch capable. It includes a GUI which provides users online measures of the spatial position, travelled distance, body speed, heading direction, relative distance to any user-defined (virtual) target and basic behavioral states. The user can flexibly create any close-loop stimulus protocol that depends on locomotion variables accessible in the output file. We further provide a wrapper in MATLAB for easy integration of PolyTouch in data acquisition and analysis pipelines.

As a proof-of-principle, we tested our close-loop system in two different place awareness paradigms. First, to provide discrete (positional) feedback, PolyTouch was used to deliver tone pulses whenever a mouse entered a user-defined virtual target zone in an open field arena. We found that the animal tended to stay shorter and moved faster in the target zone if the intensity was relatively high (>49 dB), implicating that the animal was aware of the virtual zone that was temporally coupled with sensory feedback. In our second paradigm, a continuous (distance) feedback tone was triggered with a frequency that scaled with an animal's position relative to a virtual target zone with either increasing or decreasing frequencies (range: 150 - 750 Hz). We observed that the animal adapted its exploration to maximize time spent in the portion of arena where the frequency was lowest. This approach for real-time animal tracking and rapid sensory feedback with a flight time shorter than axonal conduction latency could prove useful for a broad range of systems neuroscientists studying the principles of behavior, including but not limited to generation of sensation, perception, action, circuits of learning and memory among others.

2. Materials and Methods

2.1. Animals

Adult transgenic mice (N = 3), B6;129P2-Pvalbtm1(cr)Arbr/J were bred locally and maintained under *ad libitum* access to food and water. Animals were socially housed on a 12h light/dark cycle. Experimental procedures have been performed in accordance with the European Directive 2010/63/EU, guidelines of the Federation of European Laboratory Animal Science Associations, and the NIH Guide for the Care and Use of Laboratory Animals, and approved by an institutional ethics committee.

2.2. Animal tracking and close-loop instrumental control with PolyTouch

PolyTouch is an open-source software written in JAVA that enables animal tracking with real-time elementary behavioral classification while providing rapid feedback at millisecond resolution (see Figure 1A-C). The software consists of tracking and feedback modules, source code is made available via GitHub (https://github.com/DepartmentofNeurophysiology/PolyTouch). The user can run the software as a standalone program or call it in MATLAB (Mathworks) environment. It can be deployed in conjunction with any touch

input device, let it be a touch screen with a fixed screen resolution, mouse, touch pen or any interface that utilizes USB Touchscreen Controller (Universal) driver. In this study, we used a custom infrared touch frame (wavelength = 850 nm) where 4096 pairs of infrared emitters and detectors are placed orthogonally to each other along the four edges of a frame measuring 91 x 52.6 cm (resolution = 0.273 mm). The frame placed outside of an arena made of plexiglas, measuring 90.5 x 52.5 cm (Figure 1A; plexiglass thickness = 1 cm). Commercially, IR sensor frames are sold as "IR touch overframe", "touch frames", "multi touch frames" by various manufacturers.

The tracking algorithm makes use of open source jni4net (https://github.com/jni4net/jni4net/) and JWinPointer libraries (http://www.michaelmcguffin.com/code/JWinPointer/). It performs behavioral classification based on the temporal and directional changes in body motion. The user interface displays the current animal position (in X,Y), center-of-mass (COM) position, elapsed time, distance travelled, body speed, relative position of the (virtual) target, and basic behavioral states during data acquisition (Figure 1B). Depending on the relative distance between the ground and the sensor, different portions of the body including limbs, tail, and head can be detected. For the experiments described herein, the sensor was placed on a flat plexiglass sheet for limb detection (Figure 1C). Behavioral state identification was based on motion profiling of the animal and included discrete states of animal "moving" (body speed > 1 cm/sec), "immobile" (body < 1 cm/sec), and advancing "on the ground" or "off the ground", as the body part moves out of the 2D plane. Simple behavioral state classification allows the user to monitor animal behavior, which could also be used to trigger stimulus feedback.

The touch events are updated and exported to an ASCII file as comma separated values at an average speed of 65.5 Hz (± s.d. = 5.8 Hz). Because the data export is restricted to only those time points when the animal is in motion, the file size is kept to minimum (1 min of behavioral data is ~ 79 KB). The sampling rate of the animal position depends the CPU load of the data acquisition computer as well as the serial processing of each simultaneous touch events, a constraint of the JAVA architecture. The spatial location in a 2D plane (in pixels) and timestamp (in nanosec) of each event are stored along with the device identity (device ID, useful in case multiple sensors are used together), touch event identity (touch ID), behavioral state (mobile, immobile, on the ground, off the ground), elapsed distance (in cm) and body speed (in cm/sec). To ensure that the motion of the computer mouse does not interfere with the tracking, computer mouse is assigned to the touch ID of 1 and ignored in the rest of the processing. Note that PolyTouch is not designed for notebook computers (laptops) with touch screen displays whose resolution can be adjusted with multi touch gestures.

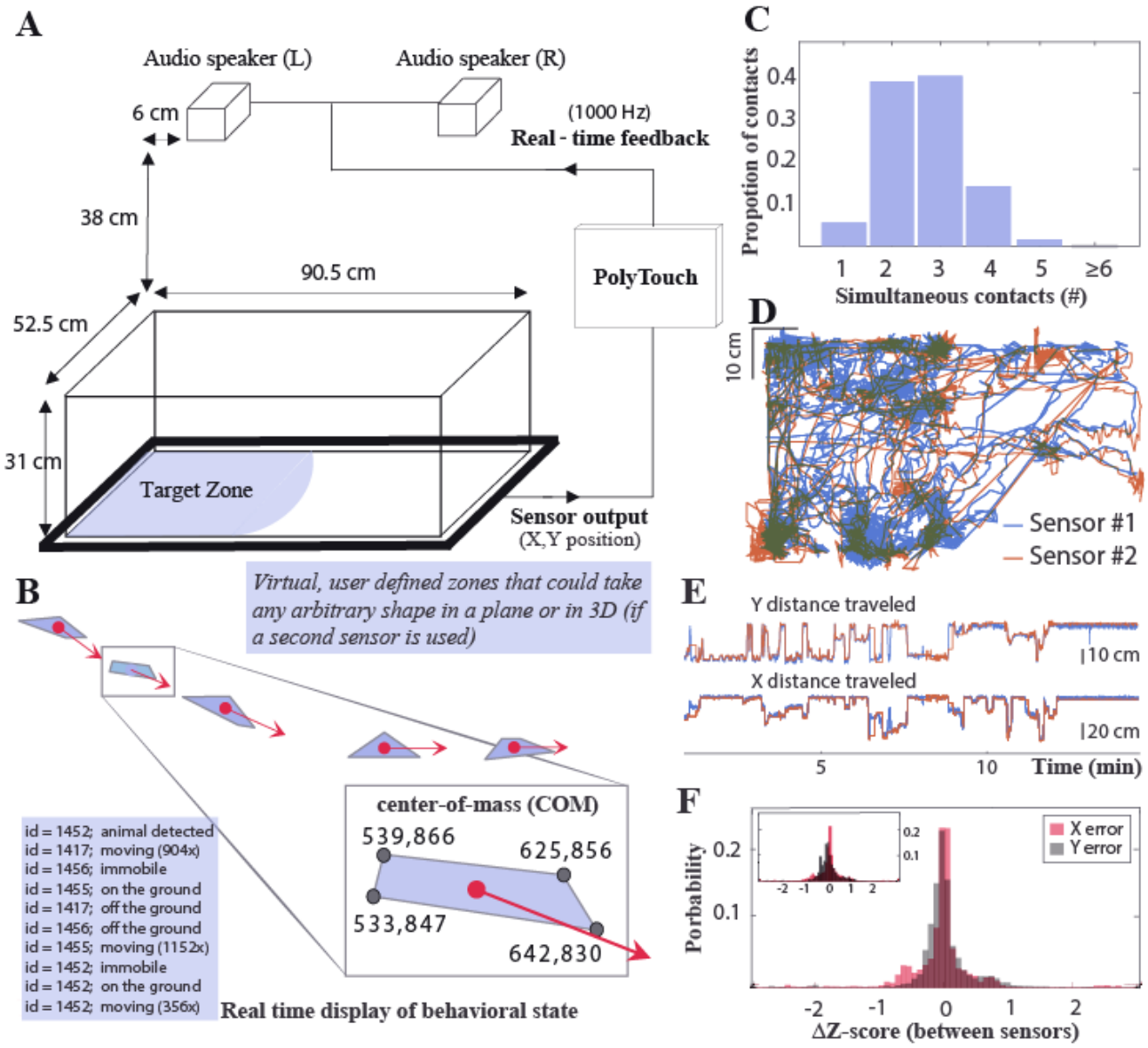

Figure 1. Experimental setup and the quantitative assessment of PolyTouch performance for motion tracking. (A) Schematic representation of the experimental setup. PolyTouch tracks animal position and provides control signals for real-time stimulus feedback. The stimulus delivery can be gated by animal behavior and animal's approach or entry to select regions of interest, called virtual target zones. **(B)** A randomly selected epoch where an animal travels along a path. Corners of the polygons denote detected single contact events. The center of mass (COM, red dots) and the vector map of body motion show the temporal change in animal position. Graphical User Interface (GUI) provides real-time information on behavioral state feedback, shown on a blue background, with contact locations, COM, elapsed time (sec), travel distance (cm), body speed (cm/sec) and distance to target zone (cm). **(C)** Histogram of touch events. Note that in a small fraction of the contact events animal's tail or head, in addition to the four limbs, can be detected. Majority of the contacts involved 2 (38.8%), 3 (40.2%) or 4 (14.1%) limbs (total number of contacts = 55207). **(D)** The error in spatial sampling as quantified using two IR touch frames and a robotic ball (see Materials and Methods for details). **(E)** The relative distance of the robot from the start position (in cm) along the x-axis (left panel) and y-axis (right panel) over time across the two sensors. **(F)** The Z-scored error difference (ΔZ-score; see Methods 2.4.3) in the COM X (red shaded bars) and Y (grey) across sensors with raw data (small upper panel) and spline fitted data for noise suppression (main panel). Mean ± standard deviation from the mean error before interpolation: -0.8 cm in X (± 3.6 cm) and 1.0 cm in Y (±3.5 cm); Mean error after interpolation: -0.3 cm in X (± 3.5 cm) and -0.2 cm in Y (± 3.4 cm).

The feedback module controls stimulus delivery (in this study only auditory) in respect to the animal position and context as determined by the user. The feedback module continuously reads the X,Y position of the last stored touch event from the external file with an average speed of 1 msec (± s.d. 1.6 msec). The feedback is delivered based on user defined scenarios. The feedback can also be provided based on calculated measures of ongoing animal movement, providing real-time feedback to the animal, e.g. in respect to its relative distance to (virtual) target. In this study we deployed two scenarios with a 1 msec average processing duration for the feedback controller: **discrete (positional) feedback** that delivers auditory stimulus with a principal frequency of 150 Hz (for the frequency spectrum; see Supplemental Figure 1) whenever the animal is in the user defined virtual target zone; **continuous (distance) feedback,** which delivers a frequency modulated tone that scales with the relative distance of the animal to the virtual target zone. PolyTouch is terminated when the user-specified session duration is reached or can be interrupted anytime if the user closes the graphical user interface (GUI).

2.2. Tracking a robotic ball (roboball)

To validate the tracking performance of PolyTouch, we simultaneously digitized the motion of a robotic ball (Sphero 2.0 ORBOTIX 3.81 cm radius) with two independent sensor frames (61.5 x 35.8 cm) and quantified the error in position estimation. The frames were stacked on top of each other (with 2 cm in between) and each connected to a separate computer to sample the position of the robot independently. To minimize the IR light scattering from the beam emitters of the other device, we rotated the top frame 180 degrees clockwise relative from the bottom frame. The robot was instructed to move according to a predefined set of heading directions (0 to 360 deg; total n directions = 72566) with a random speed between 0 to 20 cm/sec for a period of 15 minutes. The given heading directions were obtained from a behavioral session recorded previously (baseline session mouse 1).

2.3. Place avoidance task with virtual targets

To establish place awareness using a virtual target zone, animals were placed in an open field for 5 sessions. Discrete auditory feedback was provided based on the animal's position in respect to the target zone. In the first session, animals could freely explore the arena for 6 minutes in the absence of any auditory stimulation (0 dB; baseline condition). During the following three sessions, the feedback was provided whenever the animal entered the target zone. The sound intensity was increased across sessions (39 - 49 - 59 dB; low - intermediate - high tone condition, respectively; 15-20 min per session). The target zone location within the arena and the order of the sound intensity was randomly assigned between sessions and animals. In addition, during the final session, the tone (3x 39, 49, 59 dB; 10 sec each; session duration = 15-20 min) was presented pseudorandomly, independent from the animal location, to control for the sound induced changes in animal mobility. The open field was cleaned with ethanol (70%) after each session. Inter-session interval was 7 min until after the 3rd session. Afterwards it increased to 5 and 10 days for the remaining two sessions in the protocol.

The exploration chamber was placed in a sound isolation chamber (see Figure 1A). Two sound boxes (Speedlink USB speakers, Jöttenbeck GmbH, Germany) were placed on the right- and left half of the arena to

provide auditory stimuli. The setup was illuminated with white light by two strips of light emitting diode arrays placed on the chamber ceiling. The spatial resolution of tracking directly depends on the monitor size of the DAQ computer, in this study 23.6 inch monitor with 1920 x 1080 pixel, provided a spatial resolution of 0.0272 cm/pixel given the surface area of the arena (Figure 1A).

2.4. Data analysis

2.4.1 Behavioral analyses

To assess locomotion, the body position was computed as the center-of-mass (COM) of multi-touch events for each time point. The body position was resampled at 200 Hz by averaging samples within non-overlapping but consequential 5 ms bins in 2D (X,Y). If no samples fell within a bin (i.e. no motion was detected), the previous X,Y value was assigned. The resulting matrix is used to quantify the mobility duration (sec), body speed (cm/sec), and body direction (deg) as a function of time (sec) and body position (X,Y).

Mobility duration was represented as a spatial density map and computed as the time spent in a given location by dividing the exploration arena into 299 arbitrary bins (13x23 bins with 80x80 pixels/bin). Exploration duration (sec) in a given user selected (target zone, T) zone was quantified as the time spent in zone T (*versus* NT, non-target zone) per entry. Body speed over time was computed as the elapsed distance (in cm) and linearly interpolated (non-overlapping 100 msec/window) for noise suppression. Data points were excluded if body speed was > 50 cm/sec. The spatial distribution of body speed was computed as a bin-average for each given location and for zone T (*versus* NT) as described above. The animal was considered to be immobile if the body speed was < 1 cm/sec and mobile otherwise [4,52]. Body direction over time was computed as the vector angle between two subsequent COM points (see equation 1) and for each given location (7x12 bins with 160x160 pixels/bin). Body directions for immobile movements were excluded. A polar frequency histogram of body directions (bin size = 10 deg/bin) was computed as the number of observations normalized by the total number of samples per session.

$$body\ direction\ (t) = (arctan(\frac{y(t) - y(t+1)}{x(t) - x(t+1)}) * 180/pi)/\ 360$$

(equation 1)

To quantify the relative change in locomotion in T (versus NT), a locomotion modulation index (LMI) was computed as the difference in exploration duration (ED) per entry for T versus NT zone divided by the sum for each sample over time (see equation 2) after data is binned (bin size = 100 msec). Here, the exploration duration was interpolated over time using a linear smoothing method, so that LMI could be computed for each time point.

$$LMI\ (t) = \frac{EDtarget\ (t) - EDnontarget\ (t)}{EDtarget(t) + EDnontarget\ (t)}$$

(equation 2)

2.4.2 Error analyses

We performed two independent analyses for error estimation. First, to quantify the noise in spatiotemporal motion profiling, we calculated the roboball's trajectory as described above. The sampled X,Y coordinates from the second were then rotated 180 degree clockwise around its origin (X,Y = 0,0), to align the world-centric coordinates of detected motion across two sensor (IR touch) frames (see section 2.2). To remove noise caused by scattering light from the other IR touch frame samples (N = 40/143736 points for dev1; N = 6/32769 points for dev2) that laid outside the robot's radius (3.81 cm) were removed. The motion trajectories were then resampled at 200 Hz and interpolated by fitting a spline across non-overlapping 50 sec windows using fit function in MATLAB (smoothing parameter = 0.8). Data points were excluded if the traversed speed was > 50 cm/sec.

The two IR touch frames were connected to two separate computers that were not synchronized. Therefore the time series from the two sensors were aligned manually (Figure 1E). Subsequently, the error in the estimated robot position was computed as the pairwise difference between the two X,Y estimates. Finally, the data was presented as Z scores (see equation 3a-b) which showed that the variance across the sensors was within <1 standard deviation (Figure 1F) .

$$zEX(t) = \frac{EX(t) - EXmean}{EXstd}, zEY(t) = \frac{EY(t) - EYmean}{EYstd}$$

(equation 3a,b)

To determine the temporal variation in spatial estimation, we digitized the location of a stationary object (an orange) using a single IR sensor frame (session duration = 10 min). Temporal variation in spatial estimates was computed by taking the derivative of the COM (Supplemental Figure 2).

2.4.3 Statistical analyses

To assess place avoidance behaviour, the mobility and body speed were compared when the animal was in zone T versus NT across different tone stimulus conditions (0, 39, 49, 59, random dB) after testing for normality, using the Kolmogorov-Smirnov test. As both variables failed to pass the normality test, the non-parametric Mann-Whitney-U test was used to compare the median exploration duration per entry between zone T and NT for each condition as well as the median body speed. To reduce the risk of type I errors due to multiple testing, p-values were adjusted with a Bonferroni correction, with a critical p-value of 0.05 before correction. To evaluate if there was a bias in the animal's spatial trajectory, the histogram of heading direction samples was tested with a goodness-of-fit chi-square test (bin size = 10 deg, number of bins = 36, critical p-value = 0.05). A post hoc Pearson's chi-square test was used for each bin versus the sum of other bins (ratio 1:35) to determine if the observed ratio exceeded the expected ratio (number of samples / number of bins, p-values adjusted with Bonferroni correction).

3. Results

3.1. Stationary and mobile inanimate object tracking in open field

To evaluate the tracking performance of PolyTouch, we performed two independent analyses. First, we quantified the noise in spatiotemporal estimates by tracking a roboball using two IR sensor frames placed on top of each other (session duration = 15 min, Figure 1D-E) and acquired data simultaneously (see Materials and Methods for details). Noise in the raw samples was quantified as the pairwise difference of z-scores for each axes across the two sensors (Figure 1F). The mean error estimation in the X position was 0.8 cm (± standard deviation (s.d.) = 3.6 cm) and 1.0 cm in the y position (± s.d. = 3.5 cm). The proportion of samples with a significant (critical z-score = 1.96 s.d.) error estimation in the body position was 2622/169339 (1.6%) in X, and 502/169339 (0.3%) in Y. After interpolation, the mean error in X reduced to 0.3 cm (± s.d. = 3.5 cm) and 0.2 cm in Y (± s.d. = 3.4 cm). The proportion of samples with a significant error in X was 2407/169339 (1.4%), 543/169339 (0.3%) in Y. These findings show that 98.6% of contacts detected spatiotemporally well matched across sensors.

The temporal variation in the position estimate was quantified independently by tracking a stationary object (an orange) using a single IR sensor frame (session duration = 10 min). The temporal variability in COM estimates was zero pixel (Supplemental Figure 2). Taken together, our findings indicate that PolyTouch reliably estimated the position of a stationary object with a single-pixel precision. Increased error in COM estimate during object motion is likely to be due to change in the reflected light however spline fitting the raw data enables efficient denoising.

3.2. Tracking animal navigation in open field

Next, to exemplify the utility of PolyTouch for close-loop control of animal navigation, we provided tone feedback every time the animal entered a user defined virtual target zone. The training consisted of five sessions (t = 5-20 min/session). The first three sessions were delivered on the same day (average inter session interval = 7 min) and the subsequent two sessions 5 and 10 days, respectively, after the first experimental day.

Mice could freely explore the arena during the first session (t = 5 min; habituation session) without any tone feedback provided. During the subsequent three sessions, animal entry to a user defined virtual target zone triggered a discrete 150 Hz tone at 39, 49, or 59 dB (t = 15-20 min/session). During the final session 10s tone sweeps (3x per stimulus condition) were pseudo-randomly presented to decouple the stimulus presentation from the animal's location (t = 15-20 min).

Locomotion tracking showed that animals remained mobile, i.e. body speed > 1 cm/sec, on average 81% of the first session (Figure 2A-B, 2D-E). Animals tended to walk faster along the walls and center part of the arena (Figure 2F-G), and spent the most time at the four corners (Figure 2C). This stereotypical thigmotaxic navigation discontinued in the subsequent sessions as the animals habituated to the environment and became increasingly less mobile.

To quantify whether the spatial (thigmotaxic) bias in exploration is accompanied by a motor bias, we computed the body direction (Figure 2H) and trajectory of the animals (Figure 2I). The results showed that once the navigation is initiated, animals either preserved their body orientation, continuing their forward motion, or reversed their trajectory to revisit the path they took (Figure 2H). This pattern of exploration was not spatially constrained to any given portion of the arena (Figure 2I). These results suggest during open field exploration animal behavior is intrinsically driven rather than being extrinsically instructed in this simple arena.

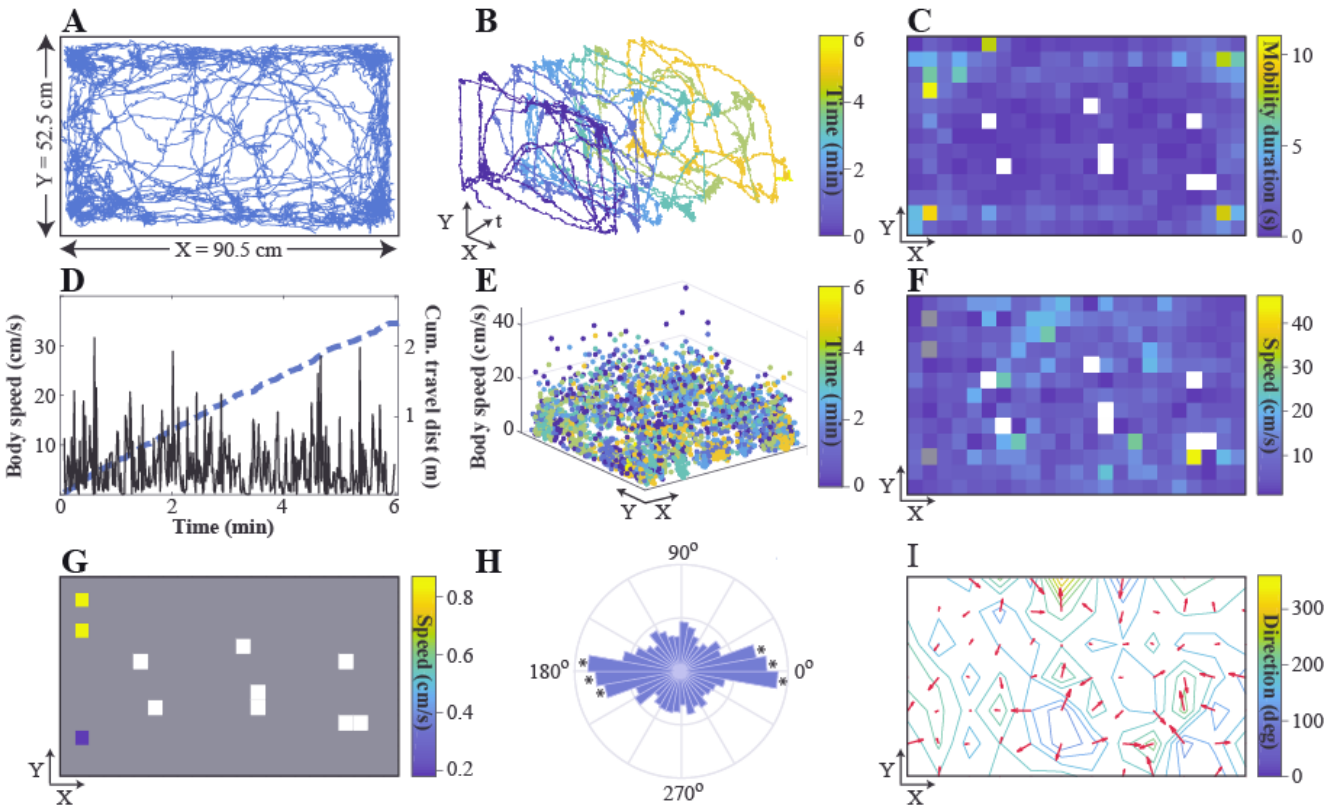

Figure 2. Open field exploration. (A) Example trajectory of one mouse (id#2) in the open field during the habituation session (no auditory feedback, session duration = 6 min). The body position is estimated as the center-of-mass (COM) of simultaneous contact points. **(B)** Same trajectory as (A), but over time. **(C)** Mobility duration (in sec; bin size = 3.93 cm/pixel). **(D)** Time resolved body speed (black) and cumulative distance traveled (blue) throughout the session. **(E)** Spatial mapping of body speed within arena across the session (spatial resolution = 0.273 mm). **(F)** Spatial distribution of body speed during animal mobility (bin size = 3.93 cm/pixel; white bins indicate never visited positions, grey bins indicate animal mobility was <1 cm/sec). **(G)** Same as in (F), but when the animal was immobile (body speed < 1 cm/sec; grey bins indicate the animal was mobile). **(H)** Polar histogram of the body direction (bin size = 10 deg) when the animal was moving (* indicates that bin significantly exceeded the expected uniform distribution with $p < 0.05$, Pearson's chi-square test). **(I)** Bin-averaged body direction (in deg) and direction gradient ($\partial F/\partial x$) from 0 deg (blue) to 360 (yellow) for each given location (bin size = 7.54 cm/pixel).

3.3. Place avoidance training with real-time positional feedback

Next, to establish an instructive control over animal navigation, we provided real-time contextual feedback. Animals rapidly learned to avoid the target zone during sessions where entry to a user defined target zone triggered a moderate intensity (~59 dB) tone (Figure 3). In this close-loop positional (discrete) feedback

training, animals first explored the entire arena (Figure 3B) with thigmotaxis (Figure 3B,C) before completely avoiding the target zone after ~7 min exposure (Figure 3B).

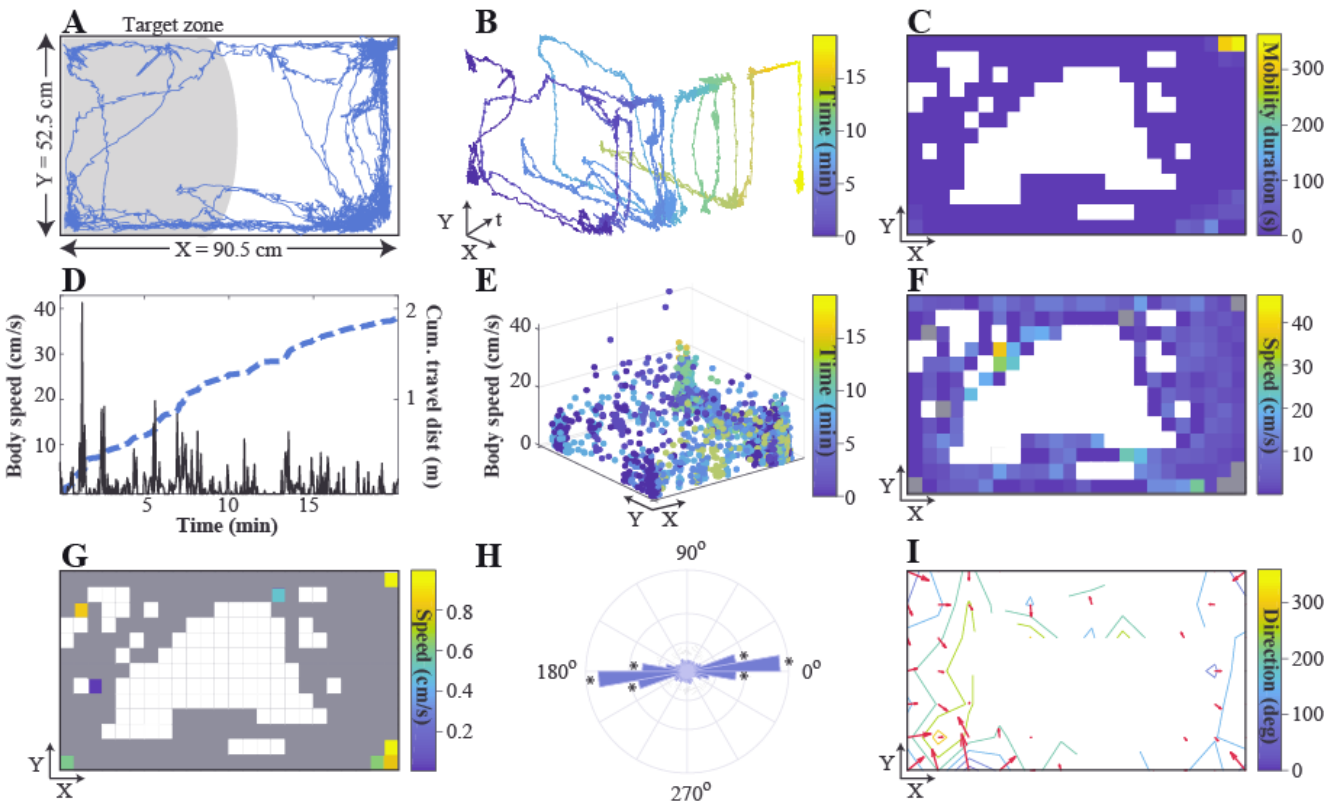

Figure 3. Place conditioning (Spatial avoidance training) with close-loop positional (discrete) feedback using virtual targets. (A) An example trajectory of one mouse (id#2, same as in Figure 2) when a discrete 59 dB tone feedback was delivered every time animal visited a user selected target zone, shaded in grey (session duration = 20 min). **(B)** Same trajectory as in (A), but over time. **(C)** Mobility duration (bin size = 3.93 cm/pixels). **(D)** Time resolved body speed and cumulative distance traveled throughout the session. **(E)** Spatial mapping of body speed within the arena throughout the session (spatial resolution = 0.273 mm). The color code represents time relapsed since the session onset. **(F)** Bin-averaged body speed when the animal was moving (body speed > 1 cm/sec) for each given location (bin size = 3.93 cm/pixel; white bins indicate never visited positions, grey bins indicate that the animal was immobile). **(G)** Same as in (F), but when the animal was immobile (body speed < 1 cm/sec; grey bins indicate the animal was mobile). **(H)** Polar histogram of the body direction (bin size = 10 deg) when the animal was moving (* indicates that bin significantly exceeded the expected uniform distribution with $p < 0.05$, Pearson's chi-square test). **(I)** Bin-averaged body direction (in deg) and direction gradient ($\partial F/\partial x$) from 0 deg (blue) to 360 (yellow) for each given location (bin size = 7.54 cm/pixel; white bins indicate never visited locations).

The positional feedback significantly reduced the overall speed of navigation (median ± 1st-3rd IQR of body speed with and without tone feedback: 0.1 cm/sec ± 0-1.8 cm/sec vs 3.6 cm/sec ± 1.1-8.9 cm/sec, Mann-Whitney-U test, $p < 0.05$) except when exploring the target zone, which was increased during target zone exploration (median ± 1st-3rd IQR of body speed in the T and NT zones: 3.5 cm/sec ± 1.0-8.4 cm/sec vs 0.2 cm/sec ± 0-2.4 cm/sec, Mann-Whitney-U test, $p < 0.05$). Notably, the observed bias in the animal's trajectory for forward and reverse-traversed motion in the baseline condition (Figure 2H) seemed to be reinforced in

close-loop conditions (Figure 3H), suggesting that discrete positional feedback might promote motion along a course.

To quantify the temporal evolution of the avoidance behavior, we calculated a locomotion modulation index (see Methods 2.4.3). The LMI index is a normalized measure of explorative behavior that could take positive or negative values. Positive values indicate that animals spend more time (Figure 4A) in the target (T) zone (Figure 4B), while negative values are measures for non-target (NT) zone exploration. The results show that in the absence of auditory feedback (Figure 4, first column) the animals explored both T and NT throughout the entire session (see Figure 5 for group analysis), without a bias towards exploration of the either zone. Low intensity auditory (39 dB) feedback did not change the exploration duration or the speed of navigation (Figure 4, second column). At higher intensities (49 and 59 dB) mobility was directed towards the non-target zone (Figure 4, third and fourth columns) as animals avoided the T zone only after one entry. After task acquisition, the avoidance behavior was generalized. Animals avoided entry and exploration of the T zone even if auditory stimulus was not coupled to the T zone entry, rather 10 sec tone sweeps were delivered randomly during exploration (Figure 4, last column).

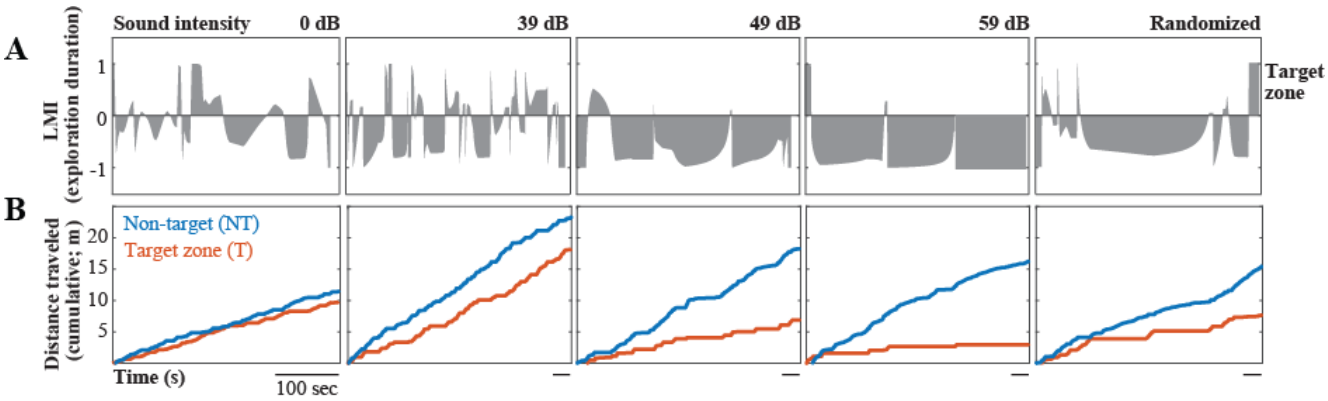

Figure 4. Temporal evolution of the place conditioning. Open field navigation was quantified in the absence of auditory feedback (baseline, 0 dB), or during auditory feedback. The feedback was provided either in a close-loop whenever the animal entered the virtual target zone, using three different tone intensities (39-49-59 dB), or as open-loop feedback, presented pseudorandomly over time (3x 39, 49, 59 dB 10 sec tone), independent from the animal's visit of the virtual target. **(A)** Locomotion modulation index (LMI) for duration of time spent in the T and NT zones. LMI = ED_T - ED_{NT} / ED_T +ED_{NT}, (see Methods 2.4.1). Positive values denote preferential exploration of the T zone, negative values NT zone. **(B)** Cumulative distance travelled across session. Data from a single representative animal.

Group analyses showed that animal mobility was modulated by both close- and open-loop auditory feedback (Figure 5). During close-loop feedback, when auditory stimulus was delivered at higher intensities, the animals explored the T zone less, avoiding the virtual target (Figure 5A; $p<0.05$, Mann-Whitney-U test), and moved faster (Figure 5B; $p<0.05$, Mann-Whitney-U test). Faster mobility was also observed during open-loop feedback (Figure 5B; $p<0.05$, Mann-Whitney-U test). Taken together results outlined in Figures 3-5 argue that place conditioning can be successfully induced during spatial avoidance training using virtual target zones as PolyTouch provides context/location specific and independent feedback. The place avoidance is rapidly induced in a single session and can be generalized across stimulus intensities.

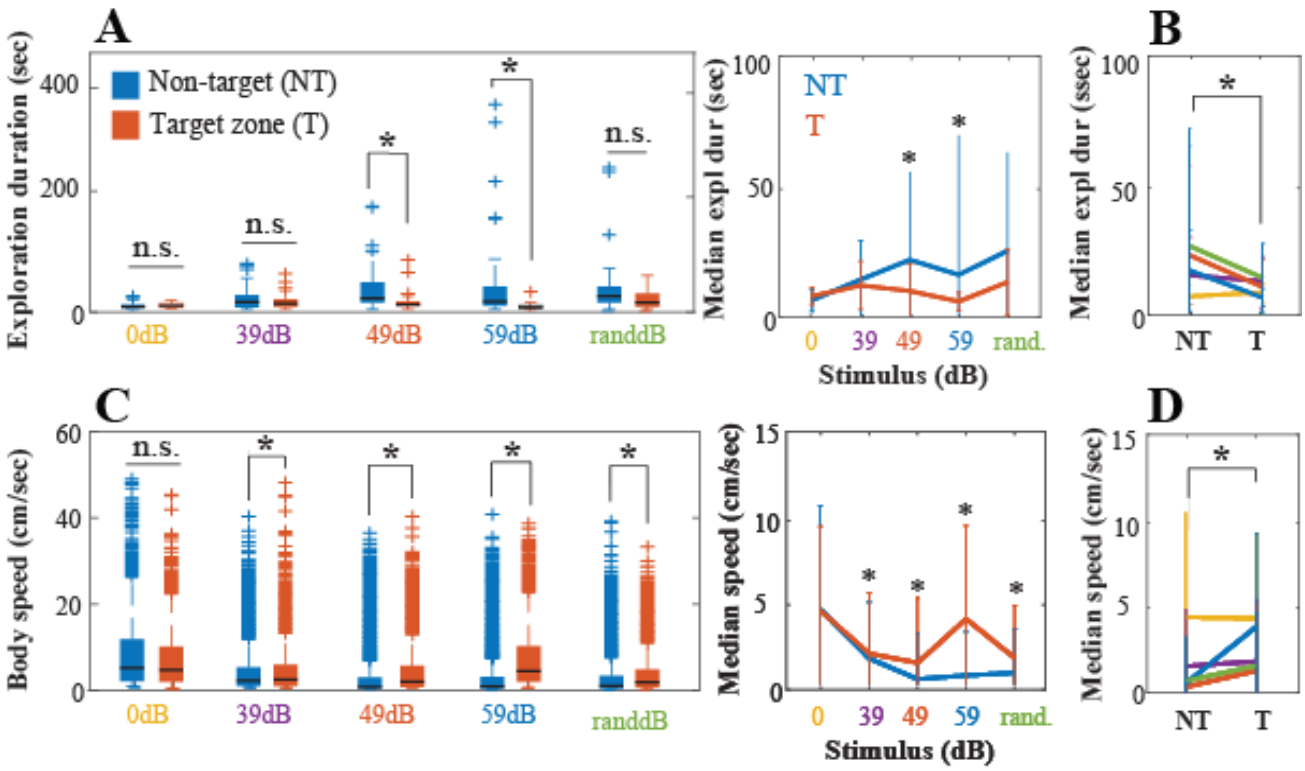

Figure 5. Comparison of animal mobility across stimulus conditions. (A) Exploration duration (ED) pooled across two mice in the randomly assigned target (T, orange) versus non-target (NT, blue) zone baseline, 39, 49, 59 and random dB tone conditions. Left panel: boxplot with median ED (black line), 1st and 3rd quartile outliers (lower and upper lines), and outliers (cross symbols). The median ED was not significantly different between the T and NT zone for the baseline (ED_T = 7.9 sec, 1st-3rd interquartile range, IQR_T = 4.5-11.8 sec; ED_{NT} = 6.3 sec, IQR_{NT} = 3.4-10.2 sec; p = 0.98), 39 dB (ED_T = 12.2 sec, IQR_T = 5.9-19.7 sec; ED_{NT} = 14.6 s, IQR_{NT} = 4.5-28.2 sec; p = 1) and random tone condition (ED_T = 13.6 sec, IQR_T = 6.3-31.3 sec; ED_{NT} = 26.1 sec, IQR_{NT} = 14.0-44.5 sec; p = 0.066), but was significantly lower in the T zone compared to NT zone for the 49 dB (ED_T = 10.0 sec, IQR_T =7.8-16.4 sec; ED_{NT} = 22.4 sec, IQR_{NT} = 13.7-52.7 sec; p = 7.3E-04) and 59 dB condition (ED_T = 5.8 sec, IQR_T = 3.0-7.7 sec; ED_{NT} = 16.5 sec, IQR_{NT} = 8.3-44.2 sec; p = 2.2E-06). **(B)** The median ED pooled across tone conditions was significantly higher lower for zone T compared to NT ($median_T$ = 9.0 sec, interquartile range (IQR_T) = 5.2-16.8 sec; $median_{NT}$ = 14.7 sec, IQR_{NT} = 6.3-31.3 sec, p = 2.4E-05). **(C)** Same as in A but for body speed (BS, cm/sec). The median BS was not significantly different between the T compared to NT zone for the baseline (BS_T = 5.1 cm/sec, IQR_T = 1.8-10.0 cm/sec; BS_{NT} = 4.9 cm/sec, IQR_{NT} = 1.5-11.9 cm/sec; p = 1). In contrast, the median BS was significantly higher for the T zone for the 39 dB (BS_T =1.9 cm/sec, IQR_T = 0.3-5.4 cm/sec; BS_{NT} = 1.6 cm/sec, IQR_{NT} = 0.2-4.7 cm/sec; p =1.1E-7), 49 dB (BS_T =1.6 cm/sec, IQR_T = 0.08-5.3 cm/sec; BS_{NT} = 0.3 cm/sec, IQR_{NT} = 0-2.7 cm/sec; p =1.3E-12), 59 dB (BS_T = 3.8 cm/sec, IQR_T = 1.3-9.4 cm/sec; BS_{NT} = 0.6 cm/sec, IQR_{NT} = 0-3.1 cm/sec; p = 8.6E-35), and random tone condition (BS_T = 1.5 cm/sec, IQR_T = 0.3-4.6 cm/sec; BS_{NT} =0.6 cm/sec, IQR_{NT} = 0.02-2.9 cm/sec; p = 2.2E-11). **(D)** The median BS pooled across tone conditions was significantly higher lower for zone T vs NT ($median_T$ = 2.2 cm/sec, interquartile range (IQR_T) = 0.3-6.1 cm/sec; $median_{NT}$ = 0.8 cm/sec, IQR_{NT} = 0-3.6 cm/sec; p = 9.8E-67). A Mann-Whitney-U test was used for all multiple comparisons (see Methods 2.5.3 for the details on statistical method selection). * denotes p<0.01.

3.4. Continuous positional feedback during open field navigation

Discrete two-state feedback provides animals binary information, e.g. whether or not they are in a target zone as implemented in Section 3.3. PolyTouch can also be used to provide higher dimensional and continuous feedback. We have implemented such a training protocol by continuously providing auditory feedback regarding an animal's relevant location to a user selected virtual target zone (Figure 6). During the habituation session a mouse explored the open field (t = 5 min) without any auditory feedback. In the next two sessions, the subject received continuous tone that increased (or decreased) in frequency (150:150:750 Hz or 750:-150:150 Hz) as it approached the target (t = 10 min/session; average inter-session interval = 5-10 min).

To determine how the animal's exploration behavior changed as a function of the distance to the target zone, we quantified the exploration duration (in sec), body speed (in cm/sec), and body direction (in deg) over time and for each zone in the open field. The walked trajectory revealed that the animal actively explored the arena during the baseline session (data not shown), with a proportion of time spent in a mobile state of 0.90 (body speed > 1 cm/sec). The animal spent most time in zone 2 (exploration duration, ED = 104.2/298.9 sec = 34.9%) and zone 5 (ED = 82.5/298.9 sec = 27.6%; Figure 6J, Supplemental Figure 7A), spending the most time at the four corners.

The body speed fluctuated across zones, but no obvious differences were observed (Supplemental Figure 7B). Similarly, the animal remained mobile in the subsequent session and spent most time in zone 2 (ED = 242.3/702 sec = 34.5%) and zone 5 (ED = 250.3 /702 sec = 35.6%; Figure 6K, Supplemental Figure 7A). Again, no obvious differences were observed in the body speed of the animal across zones (Supplemental Figure 7B). This may indicate that exploration behavior under close-loop conditions was similar to baseline conditions. Indeed, the heading direction of the animal's trajectory revealed similar frequency distributions and were non-uniformly distributed ($p < 0.05$, Pearson's chi-square test).

In comparison, after the first session of continuous positional feedback training the animal systematically alternated between mobile and immobile periods (proportion immobile = 0.56, body speed < 1 cm/sec; Figure 6A-B, D). It spent the most time exploring the zone 5 (ED = 369 /710 sec = 51.9%; Figure 6C, Supplemental Figure 7A), where he moved the slowest (Supplemental Figure 7B). The frequency distribution of the animal's heading direction was non-uniformly distributed ($p < 0.05$, goodness-of-fit chi-square test, Figure 6H). Given that the lowest frequency tone was presented in zone 5, our findings may indicate that the animal preferred to stay in the area that was coupled with the lowest sound intensity feedback.

Although we have used 5-state feedback to encode the relative position of the animal to the virtual target, the dimensionality can be increased by the PolyTouch user to match the experimental requirements. Alternatively, multiple target zones can be designated to shape animal navigation with virtual targets.

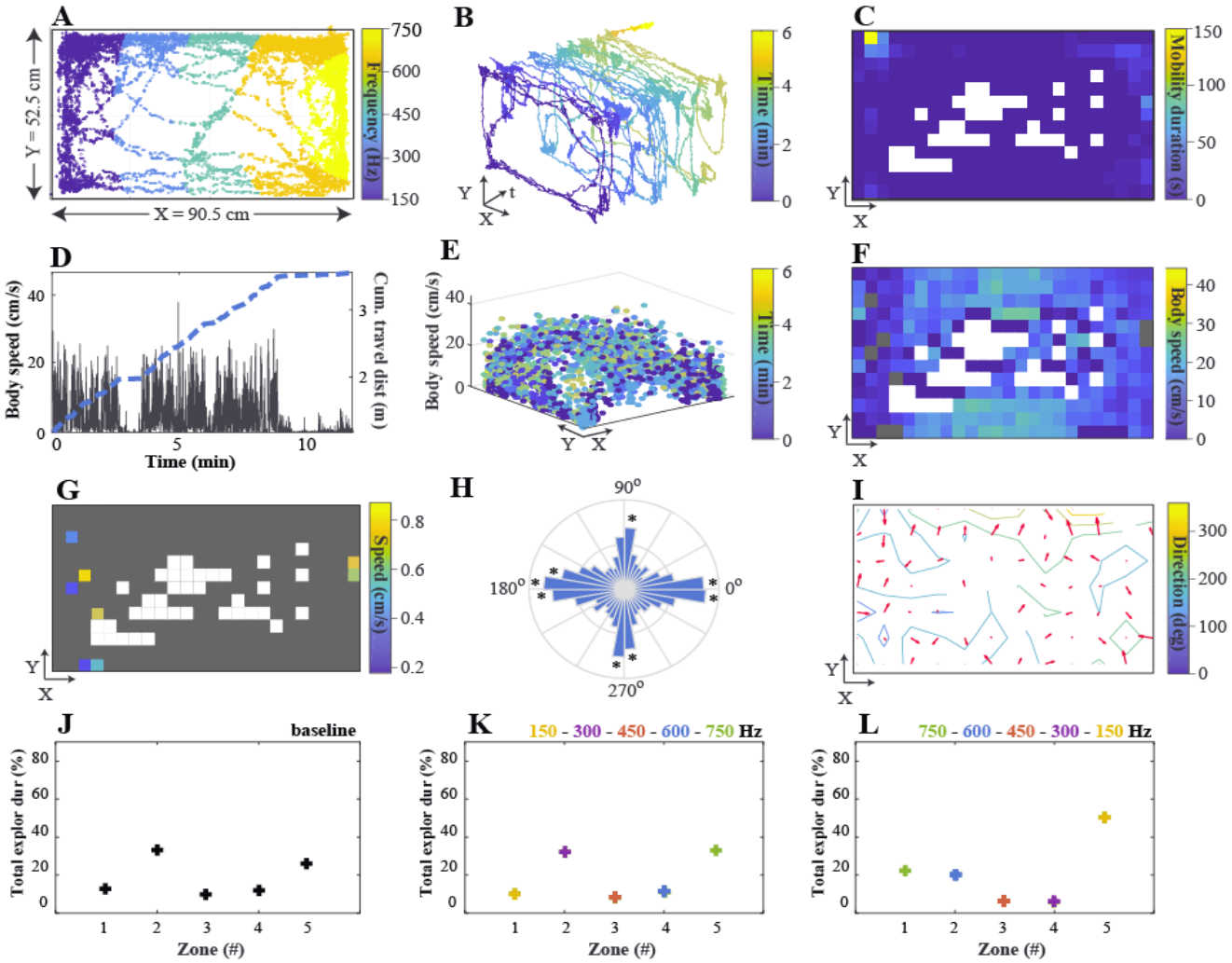

Figure 6. Locomotion activity in open field with close-loop auditory feedback. **(A)** Example trajectory of one mouse (id#3) in the open field where a continuous sine tone was given with a frequency that scaled with the distance of the animal to five different virtual target zones (session 3, session duration = 10 min). Each dot represents the center-of-mass (COM) body position**.** **(B)** Same as in (A), but over time (t, in min). **(C)** Bin-sum exploration duration (ED, in sec) for each given location in the open field (bin size = 3.93 cm/pixel; white bins indicate never visited positions). **(D)** Body speed (in cm/sec) over time (in min) after applying a linear smoothing function (non-overlapping 3sec/bin windows). **(E)** Body speed (in cm/sec) as a function of the center-of-mass position in the open field throughout the session. **(F)** Bin-averaged body speed when the animal was moving (body speed > 1 cm/sec) for each given location (bin size = 3.93 cm/pixel; white bins indicate never visited positions, grey bins indicate that the animal was immobile). **(G)** Same as in (F), but when the animal was immobile (body speed < 1 cm/sec; grey bins indicate the animal was mobile). **(H)** Polar histogram of the body direction (in deg, bin size = 10 deg) when the animal was moving. **(I)** Bin-averaged body direction (in deg) and direction gradient (`∂F/∂x`) `from 0 deg (blue) to 360 (yellow)` for each given location (bin size = 7.54 cm/pixel; white bins indicate never visited locations). **(J)** Total ED as a percentage of the session duration (in %) in each zone 1 to 5 for the baseline session (no feedback): 13.8%, 34.9%, 11.2%, 12.6% and 27.6%, respectively **(K)** Same as in (J), but for the close-loop condition where tone feedback decreased in frequency as the animal approached zone 5. Total ED as a percentage of session duration for zone 1 to 5: 10.1%, 34.5%, 8.6%, 11.2% and 35.6%, respectively **(L)** Same as (I), but where tone feedback increased in frequency as the animal approached zone 5. Total ED as a percentage of session duration for zone 1 to 5: 21.1%, 19.1%, 3.8%, 4.0% and 52.0%, respectively.

4. Discussion

PolyTouch is a novel, open source, markerless (i.e. does not require body part of animals to be tagged) tracking software with integrated feedback delivery capabilities. It continuously tracks animal locomotion while providing control signals to connected devices for close-loop control (Figure 1A). The main features of the software are (1) simultaneous tracking of multiple body parts using any IR sensor frames, connected to the data acquisition computer via the Universal USB Touchscreen Controller driver, with a temporal resolution (in this study: 66-74 Hz) and high spatial resolution (1920x1080 pixels, 0.0273 cm/pixel as deployed herein), (2) real-time feedback based context or animal position with an average communication latency of 1.0 msec, (3) low noise (temporal: ~0% ; spatial: <1.7% at 0.0273 cm pixel resolution) reconstruction of navigation over extended periods of time and (4) continuous update of the stored behavioral data with minimal memory load on the host computer resources.

PolyTouch provides users real-time visual feedback by displaying touch locations, center-of-mass (COM) body position, body speed, travelled distance, behavioral state (mobile, immobile), and distance to any user-defined virtual zone. It is fully automated and flexible, as the user can access various locomotion variables during and after data acquisition from a lightweight output file (1 min ~ 79 KB). This provides means to evaluate the occurrence, duration and timing of behavioral sequences in a standardized manner, and allows for synchronization with other experimental modules, e.g via provided MATLAB scripts for real-time data visualization, feedback control, integration with electrophysiological recordings. The recording arena can take any size, constrained only with the dimensions of the sensor frame, and could be extended to the third dimension using multiple IR sensor frames simultaneously. The open field arena can be extended with transparent walls and tunnels to create a more complex and enriched environment, which not only widens the variety of exploration behaviors that can be studied, but also benefits the animal welfare [53].

We implemented the close-loop system in two exemplary place awareness paradigms. In the first paradigm, a discrete tone was presented whenever the animal entered a user defined target zone. In this context, animals spent significantly less time and travelled faster in the target compared to non-target zone, but only if the tone intensity was sufficiently high (Figure 5A-B), indicating that place avoidance behavior emerged if the tone feedback was aversive. The tendency to avoid the target zone (which was randomized across sessions) increased with the exposure time to auditory feedback within the span of a single session (Figure 4A, 4C). This result argues that animals actively switched their place preference based on the sensory feedback within ~20 min as a result of a rapid spatial learning [54,55]. In the second paradigm, a continuous feedback about an animals' relevant distance to the target zone was provided by modulating frequency of the tone, providing real-time positional feedback. After the initial familiarization to the paradigm, the animal spent the most time in the portion of the arena where the lowest frequency stimulus was given, maximizing the distance between the target and itself (Figure 6). Taken together, we show that PolyTouch can be used to provide real-time discrete and continuous sensory (auditory) feedback to bias animal navigation with virtual targets. The virtual targets can take any 2D shape, and can be extended to 3D by using multiple sensors to track animals' elevation. The targets

can be spatially anchored in the arena (as it is implemented in the current study), or can be coupled to animals' own exploratory body movements, e.g. change in speed and direction of movement, to immobility. Inclusion of objects in the exploration arena and creating associated virtual targets can extend the utility of this approach, as auditory stimulus frequency and intensity could be modulated to create aversive contexts.

4.1. Limitations of the PolyTouch

The close-loop system of PolyTouch consists of a tracking and feedback module that run in parallel. The speed of tracking depends on the number of touch events detected simultaneously as each event is processed in series. Accordingly, the sampling rate was ~74 Hz when an immobile object (single point) was tracked compared to ~66 Hz in freely moving mice (up to 6 points tracked/mouse, see Figure 1C for the contact distribution) using a standard notebook computer with an iCore 5 Intel processor and 8GB DDR2 RAM. The sampling rate was constant within and across sessions, indicating that memory handling by PolyTouch does not interfere with the tracking performance.

Our sampling error analysis revealed a small (1.7%), not statistically significant, error in animal tracking when two frames were used to track the same animal (Figure 1F). A possible explanation for the observed errors could be that noise was introduced due to the close positioning of the sensor frames to image mouse navigation. This problem can be potentially solved by optically isolating the frames, either by use of spectral filters, light-tight materials.

PolyTouch does not currently support simultaneous tracking of multiple unrestrained animals. This is because center of mass calculation is performed in every time point ("frame") independently. When multiple animals are in close proximity this algorithm will fail to identify single animals. A Bayesian clustering approach might allow identification of the animal ID based on each animal's motion trajectory and the previous spatial distributions of individual touch events. Another solution might be to position a camera under the exploration chamber, so that a post hoc image-based analysis can be performed to assign the correct animal to touch points. Although the latter solution will limit close-loop feedback capabilities of PolyTouch to spatial feedback, as single animal behavior will not be classified in real-time for rapid feedback, the solution could be implemented with the current version of the PolyTouch.

The feedback module of PolyTouch uses the audio out jack of the computer as a communication port to deliver control signals to external devices. In this study we provided auditory feedback via connected speakers, however the control signal could take any shape, e.g. TTL.

4.2. Comparison to existing tracking systems

Compared to existing open source software for animal tracking, PolyTouch is the only software that enables rapid close-loop feedback with a flight-time of 1 ms (see Table 1 for a detailed comparison). Integration of a matrix sensor frame with wide light beam emitters (see Materials and Methods) allowed us to capture animal

locomotion with a higher spatial resolution in comparison to existing infrared beam tracking systems: 0.0273 cm (PolyTouch) versus 1.6 cm [57], 2.54 cm [58], 2.63 cm [59] and >5 cm [23,26,60].

Open source software for tracking freely moving animals							
Publication (year)	**Tracking system**	**Tracking principle**	**Main features**	**Temporal resolution**	**Real-time**	**Real-time latency**	**Algorithm flexibility**
Hamers et al.(2006)	CatWalk	IR-light sensors	High-contrast imaging of footprints with a frustrated total internal reflection (FTIR)-based sensor system coupled to a CCD camera	50-60 fps	no	N/A	Semi-automated: requires initial manual marking of footprints
Machado et al.(2015)	MouseLoco	Videography	Offline 3D markerless tracking of whole-body, limbs, head, tail with automated behavioral classification	400 fps	no	N/A	Fully automated; posthoc automated classification of behavioral events; Synchronization with physiology data (BONSAI)
Mendes et al.(2015)	MouseWalker	IR-light sensors, videography	High-contrast imaging of footprints and whole-body with a frustrated total internal reflection (FTIR)-based sensor system coupled to a high-speed camera	250 fps	no	N/A	Fully automated
Del Rosso et al. (2017)	ratCAVE	Videography	3D tracking of head position in freely moving rats with close-loop visual feedback in a virtual reality system	240-360 fps	yes	15 ms	Fully automated; real-time calibration of head position and rotation to image projector; no training required for VR setup
Nashaat et al.(2017)	PIXY	Videography	Online and offline color-based tracking of whole-body, limbs, head and whiskers using a hybrid camera system. Real-time color frames are synchronized with replayed frames obtained at high speed	150 fps high-speed camera; 25-50 Hz Pixy color camera	yes	30 ms	Fully automated; Inexpensive; includes wrapper for data processing (PixyMon software)
Saxena et al.(2018)	PiCamera	Videography	Tracking of whole-body movements in large arenas (2.43x1.82m) using a scalable camera system	30 Hz	no	N/A	Fully automated
Lim & Celikel (2018)	PolyTouch	IR-light sensors	Online tracking of body position using a low-level GUI-based multi-touch interface with real-time stimulation. Markerless, inexpensive, light/dark conditions.	> 65.5 Hz	yes	1 ms	Fully automated; Inexpensive; cross-platform; runs as standalone; includes wrapper for MATLAB to automate data acquisition, analysis and visualization

In terms of processing speed, modern close-loop systems trigger feedback within 3-40 ms for neural data [10,12] and 12-50 ms for behavioral data [14,15,41,56,57]. PolyTouch can be used to control neural activity based on animal behavior at a temporal scale faster than synaptic communication along sensory pathways [58–63], and thus could be used to create artificial sensory and motor feedback in the context of rapidly evolving behavioral computations [42,64].

In recent years, many researchers have benefitted from an increase in available open-source platforms, including OpenEphys [10], BONSAI [9], NeuroRighter [65] and RTXI [66]. PolyTouch compliments the functionality of these platforms by providing rapid (within 1 ms) close-loop feedback based on animal behavior. Although our system supports data streaming of behavior to a multitude of downstream devices, it will (1) require manual coding by the user to add new threads of execution and (2) compromise in speed of processing with each extension due to its dependency on the resource utilization of the data acquisition computer (DAC). The latter issue can be solved by running PolyTouch on a separate DAC.

4.3. Future directions

PolyTouch is a flexible software whose functionality can be further improved via extension packages. To support detection of additional behaviors, such as rearing and grooming, the recording range can be extended by positioning multiple sensor frames on top of each other, so that horizontal as well as vertical movements are monitored. The user will be able to easily group locomotion data according to the position of the frame, since our software saves the device identity for each touch input in the output file. For specific behaviors that require manual observation (e.g. grooming, scratching), a future release will include the possibility for the user to report events by means of a specific key press during data acquisition.

As an extension pack, a robotic command module is currently under development that will allow users to control a robot a Sphero robot (ORBOTIX) in close-loop based on the animal's spatial trajectory to study robot-animal interactions [17,67], foraging behavior with predator-prey interactions [18,68,69] and guided spatial learning in complex navigation tasks [70]. We hope this free, open-source, fully automatized tracking software will provide users with an alternative low-cost method to track animal behavior and close-loop control of brain and behavior.

Supplementary Figures

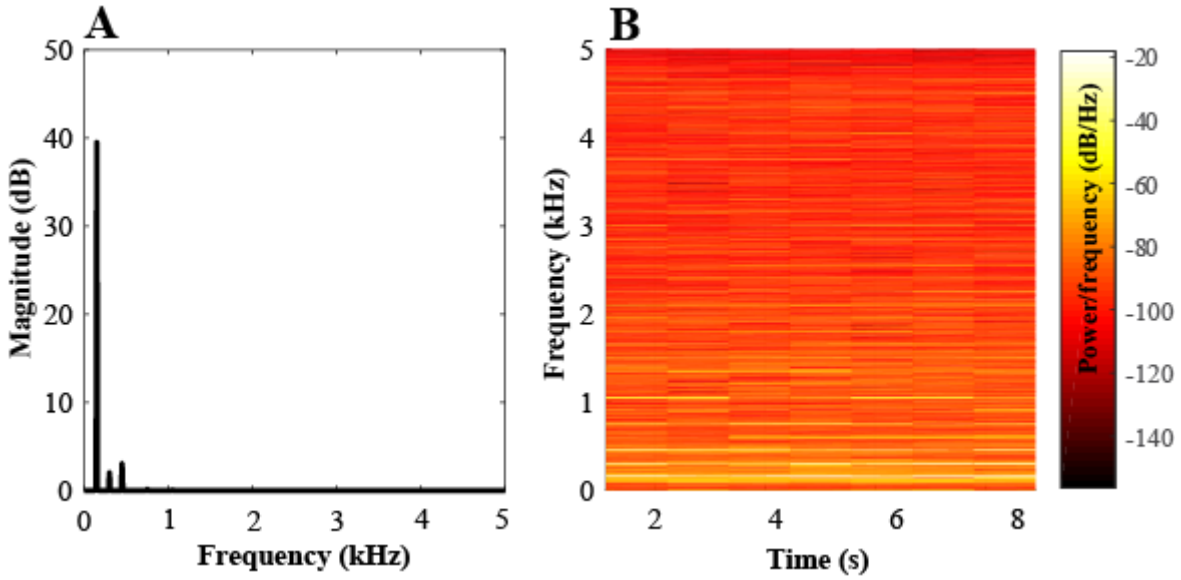

Supplemental Figure 1. Spectral analysis of sample tone stimulus. **(A)** Single-sided frequency spectrum of a 150 Hz sine wave tone (60 dB) played from two external audio speakers (frequency in kHz, sample duration = 15 sec). A fast fourier transform was computed on the original sound sample and confirmed that the principal frequency was 150 Hz with a magnitude of ~40 (frequency resolution = 10 Hz). The frequency window was limited to 0 to 5 kHz to show relevant frequency peaks. **(B)** Spectrogram of the sound sample described in (A) with frequency (in kHz) over time (in sec) using a short-term fourier transform with 50% overlap between adjacent windows (n windows = 8), where colors indicate the power per frequency (in dB/Hz).

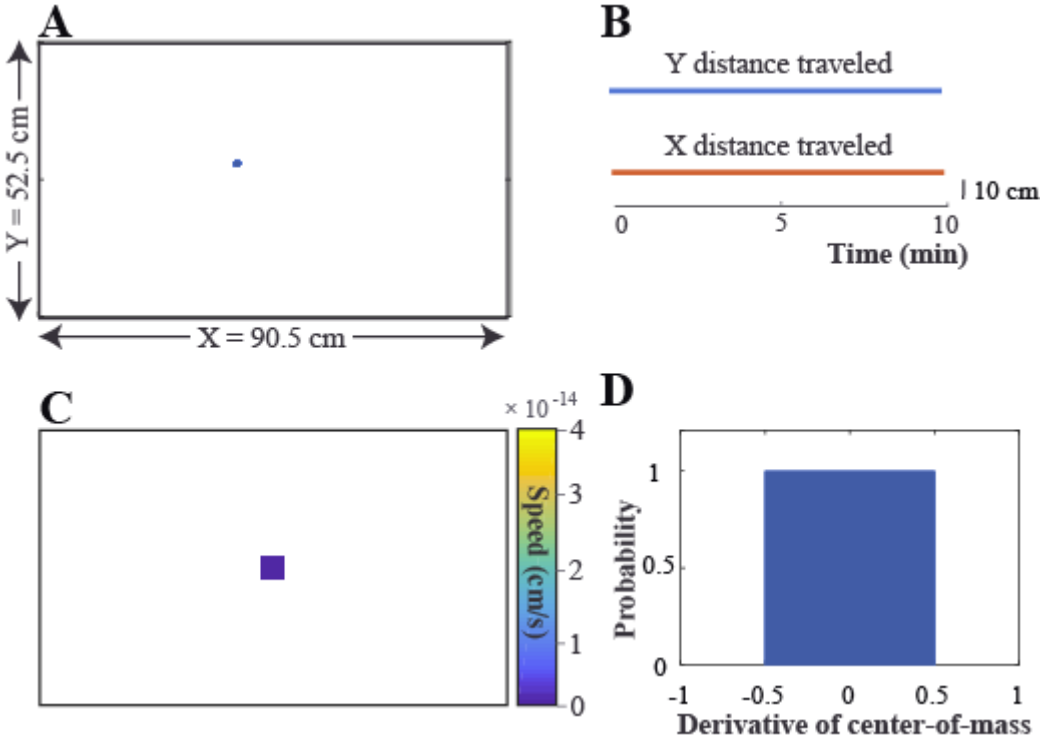

Supplemental Figure 2. Stationary object tracking in the open field. To evaluate the tracking performance of PolyTouch, we tracked a stationary object (an orange) for error estimation of the spatial x,y estimates. **(A)** Spatial trajectory of the object in the open field shows that a single x,y point (x = 788, y = 557, blue dot) was detected (session duration = 10 min; spatial resolution = 0.273 mm). **(B)** The x,y coordinates over time (in min) reveal that the object position remained constant over time. **(C)** Bin-averaged body speed (in cm/sec) for each given location in the open field (bin size = 3.93 cm/pixels). White bins indicate that the object was not detected in said bin. The average body speed of the immobile object was 0 cm/sec. **(D)** Histogram of the derivative of center-of-mass object position reveals zero spatial variation at a single-pixel resolution.

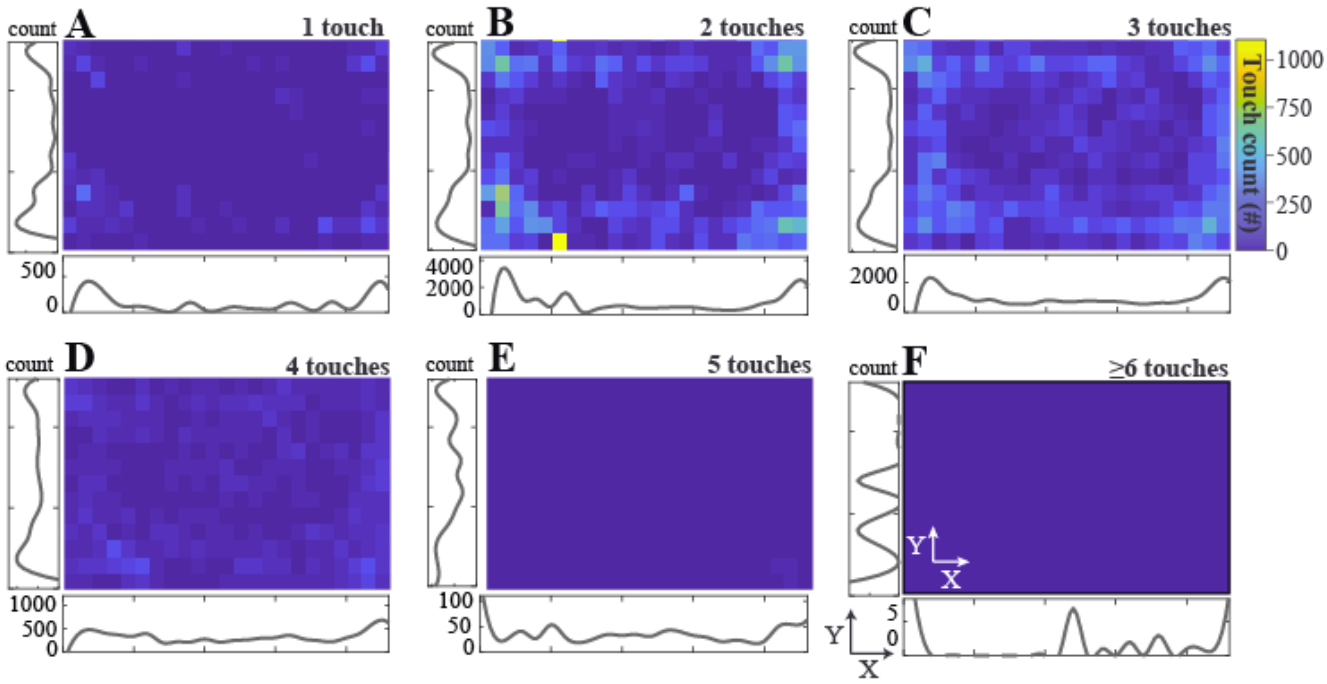

Supplemental Figure 3. Density of multi-touch events as a function of body position (animal 2). (A) Total number of single-touch events (n = 2980) spatially binned as a function of the body position in the open field (bin size = 80x80 pixels) for an example session of animal 2 during the baseline condition (0 dB; session duration = 6 min). Adjacent density plots of touch events (counts) along the x- and y-axis. **(B)** Same as (A) for touch events where 2 coincident touches were detected (n = 21444). **(C)** Same as (A) for touch events where 3 simultaneous touches were detected (n = 22194). **(D)** Same as (A) for touch events where 4 coincident touches were detected (n = 7768). **(E)** Same as (A) for touch events where 5 coincident touches were detected (n = 790). **(F)** Same as (A) for touch events where ≥6 coincident touches were detected (n 6-touches = 24, n 7-touches = 7).

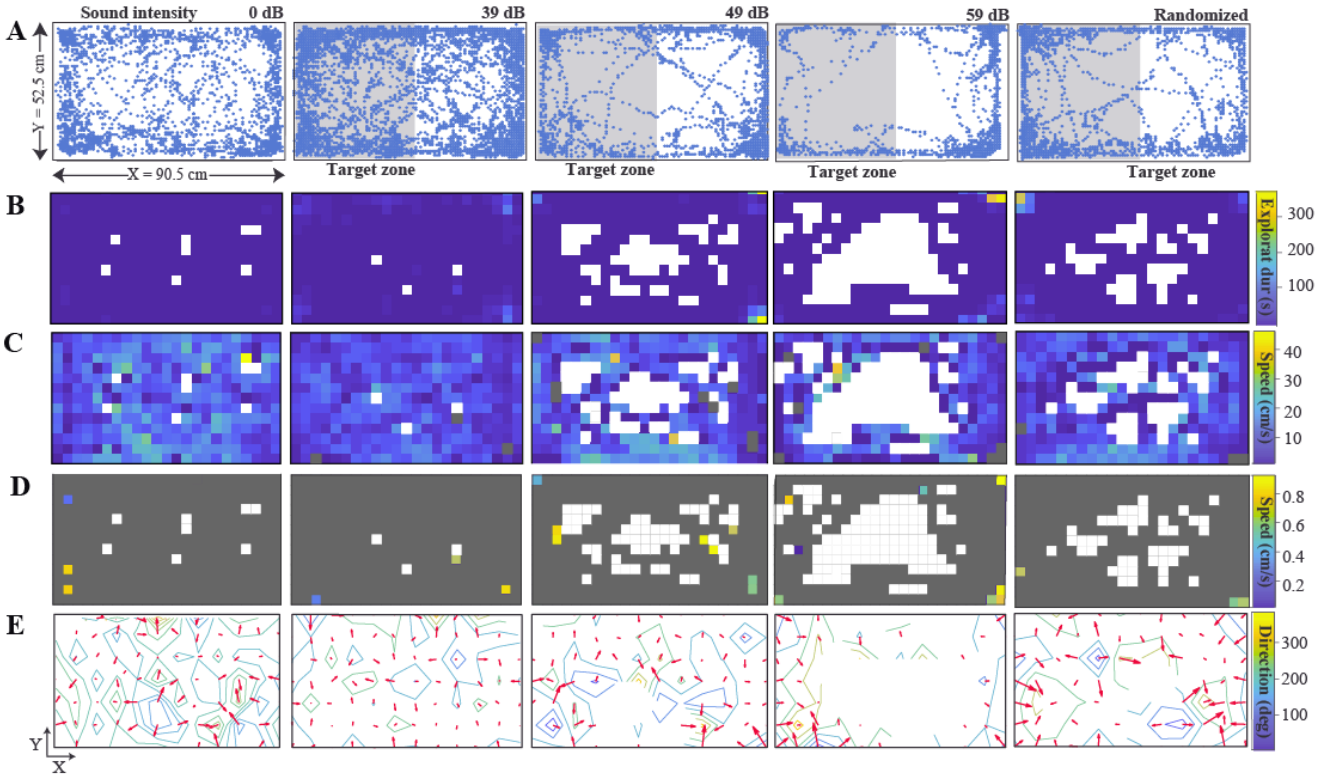

Supplemental Figure 4. Locomotion activity in open field with discrete close-loop feedback (animal 1). (A) Trajectory of animal 1 in open field arena for 5 different stimulus conditions: no feedback when the animal was in the target (T grey) zone (0 dB, session duration = 6 min, left panel), auditory feedback when the animal was in the T zone (39, 49, 59 dB discrete tone, middle 3 panels), or random feedback given pseudorandomly over time (3x 39, 49, 59 dB 10s tone, right panel). The position is the centre-of-mass of coincident multi-touches (bin size = 0.273 mm/pixel). **(B)** Bin-summed exploration duration (in sec) for each given location in the open field (bin size = 80x80 pixels) across stimulus conditions. White bins indicate never visited positions. **(C)** The bin-averaged body speed (BS, in cm/sec) for each given location when the animal was mobile (BS > 1 cm/sec) across stimulus conditions. White bins indicate never visited places and grey bins indicate that the animal was immobile (BS < 1 cm/sec). **(D)** Same as (C), but when the animal was immobile. Grey bins indicate that the animal was mobile. **(E)** Bin-averaged body directions (in deg, red arrow) and direction gradient (`∂F/∂x) from 0 (blue) to 360 (yellow) deg` for each given location across stimulus conditions (bin size = 7.54 cm/pixel; white bins indicate never visited locations).

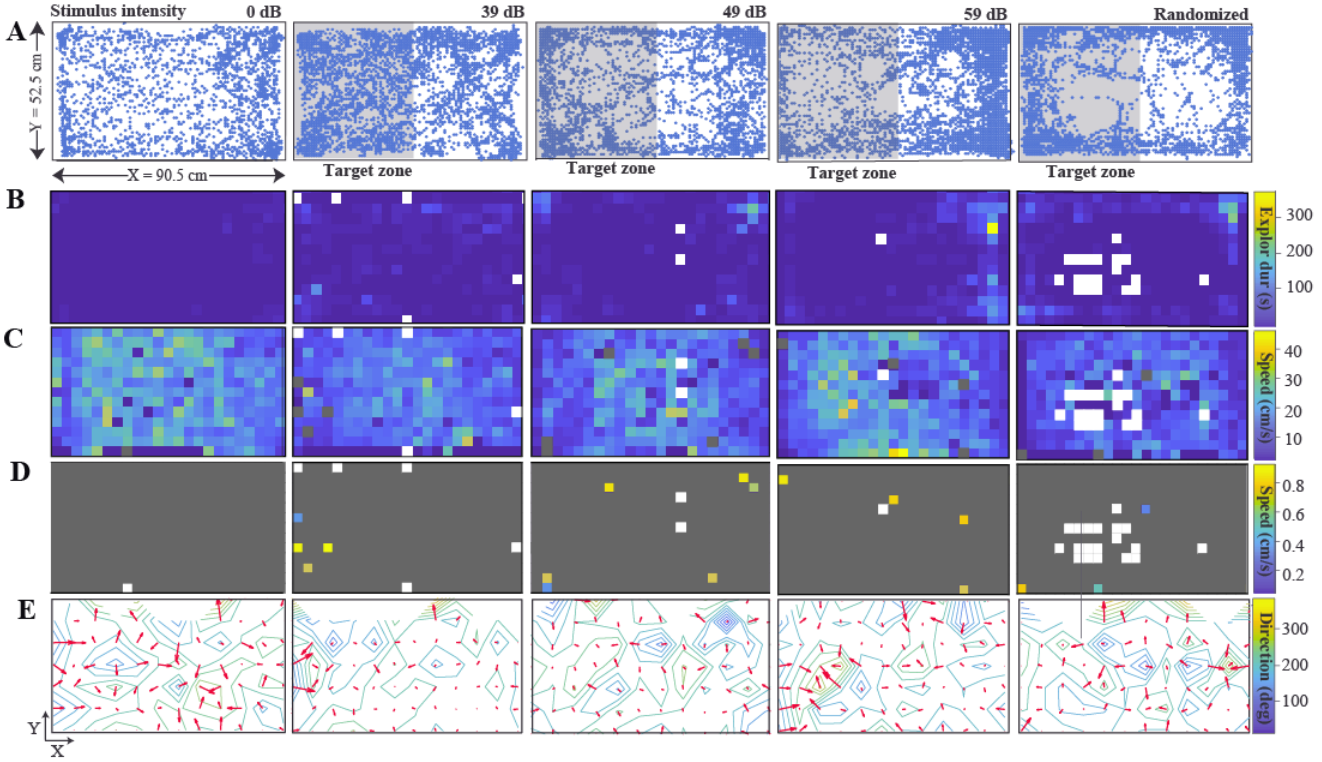

Supplemental Figure 5. Locomotion activity in open field with discrete close-loop feedback (animal 2). (A) Trajectory of animal 2 in open field arena for 5 different stimulus conditions: no feedback when the animal was in the target (T grey) zone (0 dB, session duration = 6 min, left panel), auditory feedback when the animal was in the T zone (39, 49, 59 dB discrete tone, middle 3 panels), or random feedback given pseudorandomly over time (3x 39, 49, 59 dB 10s tone, right panel). The position is the centre-of-mass of coincident multi-touches (bin size = 0.273 mm/pixel). **(B)** Bin-summed exploration duration (in sec) for each given location in the open field (bin size = 80x80 pixels) across stimulus conditions. White bins indicate never visited positions. **(C)** The bin-averaged body speed (BS, in cm/sec) for each given location when the animal was mobile (BS > 1 cm/sec) across stimulus conditions. White bins indicate never visited places and grey bins indicate that the animal was immobile (BS < 1 cm/sec). **(D)** Same as (C), but when the animal was immobile. Grey bins indicate that the animal was mobile. **(E)** Bin-averaged body directions (in deg, red arrow) and direction gradient (∂F/∂x) from 0 (blue) to 360 (yellow) deg for each given location across stimulus conditions (bin size = 7.54 cm/pixel; white bins indicate never visited locations).

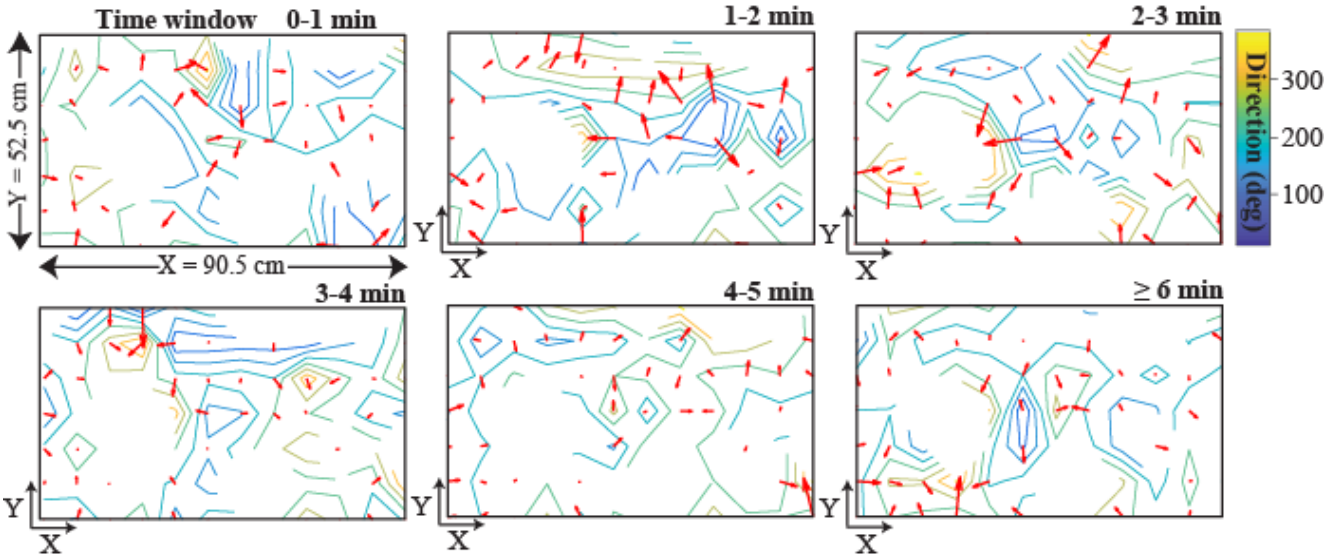

Supplemental Figure 6. Vector map of body directions in open field for sequential time windows (animal 2). Bin-averaged body direction (red arrow) and direction gradient (∂F/∂x) from 0 to 360 deg of animal 2 during baseline conditions for subsequent 1-minute epochs (no feedback, session duration = 6 min, bin size = 7.54 cm/pixel, white bins indicate never visited locations).

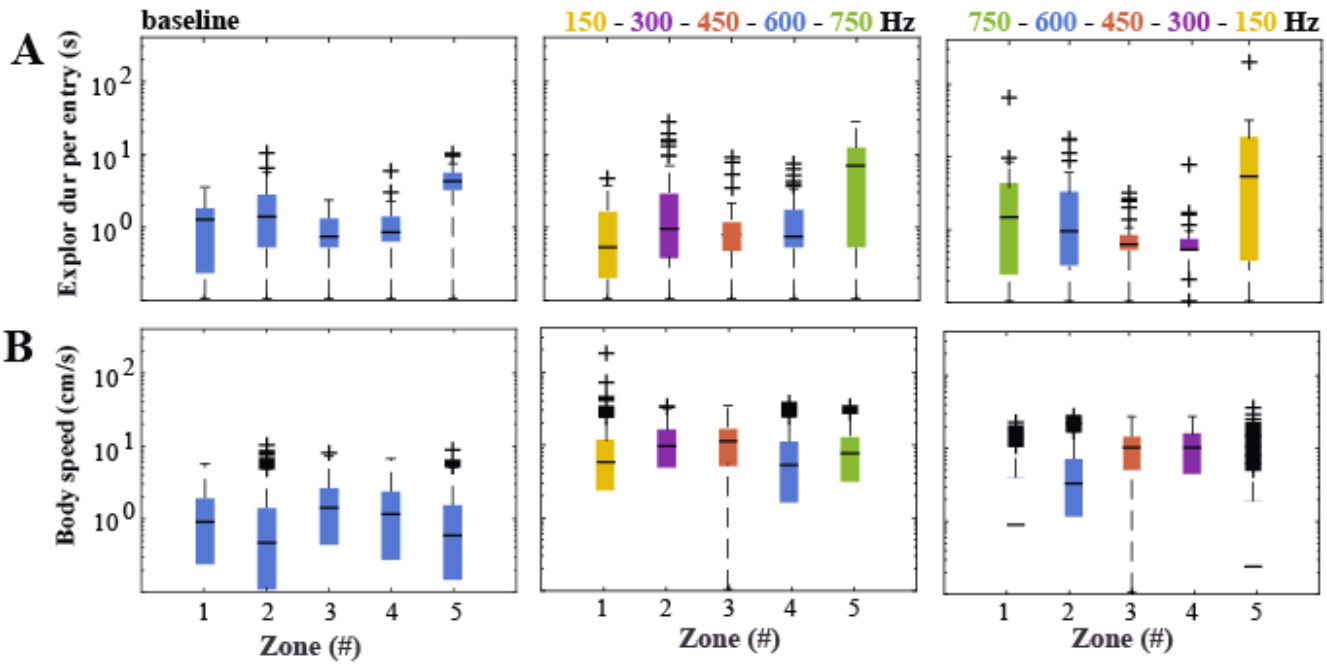

Supplemental Figure 7. Locomotion activity in open field with continuous close-loop feedback (animal 3). **(A)** Exploration duration per entry (ED, in sec) of one animal to 5 virtual zones (z1-z5) in the open field for 3 stimulus conditions: no feedback (0 dB, baseline session, session period = 5 min, left panel), feedback given as a continuous sine tone with a frequency that increased (middle panel) or decreased (right panel) with the distance of the animal relative to zone 1 (ascending frequencies: 150, 300, 450, 600, 750 Hz, descending frequencies: 750, 600, 450, 300, 150 Hz, session period = 20 min/session). Boxplot with median ED (black line), 1st and 3rd quartile outliers (lower and upper lines), and outliers (cross symbols). Left panel: median ET_{Z1} = 1.2 s, 1st-3rd interquartile range (IQR_{Z1}) = 0.2-1.7 s; median ET_{Z2} = 1.3 s, IQR_{Z2} = 0.5-2.6 s; median ET_{Z3} = 0.7 s, IQR_{Z3} = 0.5-1.2 s; median ET_{Z4} = 0.8 s, IQR_{Z4} = 0.6-1.3 s; median ET_{Z5} = 4.0 s, IQR_{Z5} = 3.1-5.1 s. Middle panel: median ET_{Z1} = 0.5 s, IQR_{Z1} = 0.2-1.6 s; median ET_{Z2} = 0.9 s, IQR_{Z2} = 0.4-2.8 s; median ET_{Z3} = 0.75 s, IQR_{Z3} = 0.5-1.2 s; median ET_{Z4} = 0.7 s, IQR_{Z4} = 0.5-1.6 s; median ET_{Z5} = 6.4 s, IQR_{Z5} = 0.5-11.4 s. Right panel: median ET_{Z1} = 1.6 s, IQR_{Z1} = 0-6.4 s; median ET_{Z2} = 5.4 s, IQR_{Z2} = 2.1-11.0 s; median ET_{Z3} = 15.3 s, IQR_{Z3} = 8.0-21.0 s; median ET_{Z4} = 15.3 s, IQR_{Z4} = 6.9-22.3 s; median ET_{Z5} = 0.47 s, IQR_{Z5} = 0-3.2 s. **(B)** Same as (A), but for the body speed (BS, in cm/sec). Left panel: median BS_{Z1} = 10.2 cm/s, IQR_{Z1} = 4.4-16.2 cm/s; median ET_{Z2} = 6.8 cm/s, IQR_{Z2} = 2.7-13.3 cm/s; median ET_{Z3} = 13.5 cm/s, IQR_{Z3} = 6.5-19.8 cm/s; median ET_{Z4} = 11.8 cm/s, IQR_{Z4} = 4.8-18.5 cm/s; median ET_{Z5} = 7.8 cm/s, IQR_{Z5} = 3.2-14.1 cm/s. Middle panel: median ET_{Z1} = 7.1 cm/s, IQR_{Z1} = 2.9-12.7 cm/s; median ET_{Z2} = 4.8 cm/s, IQR_{Z2} = 1.3-10.6 cm/s; median ET_{Z3} = 10.7 cm/s, IQR_{Z3} = 5.0-17.1 cm/s; median ET_{Z4} = 9.1 cm/s, IQR_{Z4} = 4.5-15.5 cm/s; median ET_{Z5} = 5.4 cm/s, IQR_{Z5} = 2.0-10.7 cm/s. Right panel: median ET_{Z1} = 1.6 cm/s, IQR_{Z1} = 0-6.4 cm/s; median ET_{Z2} = 5.4 cm/s, IQR_{Z2} = 2.1-11.0 cm/s; median ET_{Z3} = 15.3 cm/s, IQR_{Z3} = 8.0-21.0 cm/s; median ET_{Z4} = 15.3 cm/s, IQR_{Z4} = 6.9-22.3 cm/s; median ET_{Z5} = 0.5s, IQR_{Z5} = 0-3.2 cm/s.

5. References

[1] Freudenberg F, Resnik E, Kolleker A, Celikel T, Sprengel R and Seeburg P H 2016 Hippocampal GluA1 expression in Gria1-/- mice only partially restores spatial memory performance deficits. *Neurobiol. Learn. Mem.* **135** 83–90

[2] Freudenberg F, Marx V, Seeburg P H, Sprengel R and Celikel T 2013 Circuit mechanisms of GluA1-dependent spatial working memory. *Hippocampus* **23** 1359–66

[3] Freudenberg F, Marx V, Mack V, Layer L E, Klugmann M, Seeburg P H, Sprengel R and Celikel T 2013 GluA1 and its PDZ-interaction: a role in experience-dependent behavioral plasticity in the forced swim test. *Neurobiol. Dis.* **52** 160–7

[4] Celikel T, Marx V, Freudenberg F, Zivkovic A, Resnik E, Hasan M T, Licznerski P, Osten P, Rozov A, Seeburg P H and Schwarz M K 2007 Select overexpression of homer1a in dorsal hippocampus impairs spatial working memory. *Front. Neurosci.* **1** 97–110

[5] Ahissar E and Assa E 2016 Perception as a closed-loop convergence process. *elife* **5**

[6] El Hady A 2016 Online Event Detection Requirements in Close-loop Neuroscience *Closed Loop Neuroscience - Ahmed El Hady - Google Boeken* pp 81–8

[7] Roth E, Sponberg S and Cowan N J 2014 A comparative approach to closed-loop computation. *Curr. Opin. Neurobiol.* **25** 54–62

[8] Black C, Voigts J, Agrawal U, Ladow M, Santoyo J, Moore C and Jones S 2017 Open Ephys electroencephalography (Open Ephys + EEG): a modular, low-cost, open-source solution to human neural recording. *J. Neural Eng.* **14** 035002

[9] Lopes G, Bonacchi N, Frazão J, Neto J P, Atallah B V, Soares S, Moreira L, Matias S, Itskov P M, Correia P A, Medina R E, Calcaterra L, Dreosti E, Paton J J and Kampff A R 2015 Bonsai: an event-based framework for processing and controlling data streams. *Front. Neuroinformatics* **9** 7

[10] Siegle J H, López A C, Patel Y A, Abramov K, Ohayon S and Voigts J 2017 Open Ephys: an open-source, plugin-based platform for multichannel electrophysiology. *J. Neural Eng.* **14** 045003

[11] Martinez D, Clément M, Messaoudi B, Gervasoni D, Litaudon P and Buonviso N 2018 Adaptive quantization of local field potentials for wireless implants in freely moving animals: an open-source neural recording device. *J. Neural Eng.* **15** 025001

[12] Ciliberti D and Kloosterman F 2017 Falcon: a highly flexible open-source software for closed-loop neuroscience. *J. Neural Eng.* **14** 045004

[13] Laxpati N G, Mahmoudi B, Gutekunst C-A, Newman J P, Zeller-Townson R and Gross R E 2014 Real-time in vivo optogenetic neuromodulation and multielectrode electrophysiologic recording with NeuroRighter. *Front. Neuroengineering* **7** 40

[14] Buccino A P, Lepperød M E, Dragly S-A, Häfliger P, Fyhn M and Hafting T 2018 Open source modules for tracking animal behavior and closed-loop stimulation based on Open Ephys and Bonsai. *J. Neural Eng.* **15** 055002

[15] Liberti W A, Perkins L N, Leman D P and Gardner T J 2017 An open source, wireless capable miniature microscope system. *J. Neural Eng.* **14** 045001

[16] Paulk A C, Kirszenblat L, Zhou Y and van Swinderen B 2015 Closed-Loop Behavioral Control Increases Coherence in the Fly Brain. *J. Neurosci.* **35** 10304–15

[17] Kim C, Ruberto T, Phamduy P and Porfiri M 2018 Closed-loop control of zebrafish behaviour in three dimensions using a robotic stimulus. *Sci. Rep.* **8** 657

[18] Choi J-S and Kim J J 2010 Amygdala regulates risk of predation in rats foraging in a dynamic fear environment. *Proc Natl Acad Sci USA* **107** 21773–7

[19] Paz J T, Davidson T J, Frechette E S, Delord B, Parada I, Peng K, Deisseroth K and Huguenard J R 2013 Closed-loop optogenetic control of thalamus as a tool for interrupting seizures after cortical

injury. *Nat. Neurosci.* **16** 64–70

[20] Krook-Magnuson E, Armstrong C, Bui A, Lew S, Oijala M and Soltesz I 2015 In vivo evaluation of the dentate gate theory in epilepsy. *J Physiol (Lond)* **593** 2379–88

[21] O'Connor D H, Hires S A, Guo Z V, Li N, Yu J, Sun Q-Q, Huber D and Svoboda K 2013 Neural coding during active somatosensation revealed using illusory touch. *Nat. Neurosci.* **16** 958–65

[22] Siegle J H and Wilson M A 2014 Enhancement of encoding and retrieval functions through theta phase-specific manipulation of hippocampus. *elife* **3** e03061

[23] Clarke R L, Smith R F and Justesen D R 1985 An infrared device for detecting locomotor activity *Behavior Research Methods, Instruments, & Computers* **17** 519–25

[24] Fowler S C, Birkestrand B R, Chen R, Moss S J, Vorontsova E, Wang G and Zarcone T J 2001 A force-plate actometer for quantitating rodent behaviors: illustrative data on locomotion, rotation, spatial patterning, stereotypies, and tremor. *J. Neurosci. Methods* **107** 107–24

[25] McLelland A E, Winkler C E and Martin-Iverson M T 2015 A simple and effective method for building inexpensive infrared equipment used to monitor animal locomotion. *J. Neurosci. Methods* **243** 1–7

[26] Heredia-López F J, May-Tuyub R M, Bata-García J L, Góngora-Alfaro J L and Alvarez-Cervera F J 2013 A system for automatic recording and analysis of motor activity in rats. *Behav. Res. Methods* **45** 183–90

[27] Khroyan T V, Zhang J, Yang L, Zou B, Xie J, Pascual C, Malik A, Xie J, Zaveri N T, Vazquez J, Polgar W, Toll L, Fang J and Xie X 2012 Rodent motor and neuropsychological behaviour measured in home cages using the integrated modular platform SmartCage™. *Clin. Exp. Pharmacol. Physiol.* **39** 614–22

[28] Genewsky A, Heinz D E, Kaplick P M, Kilonzo K and Wotjak C T 2017 A simplified microwave-based motion detector for home cage activity monitoring in mice. *J. Biol. Eng.* **11** 36

[29] Heckman J J, Proville R, Heckman G J, Azarfar A, Celikel T and Englitz B 2017 High-precision spatial localization of mouse vocalizations during social interaction. *Sci. Rep.* **7** 3017

[30] Heckman J, McGuinness B, Celikel T and Englitz B 2016 Determinants of the mouse ultrasonic vocal structure and repertoire. *Neurosci. Biobehav. Rev.* **65** 313–25

[31] Bains R S, Wells S, Sillito R R, Armstrong J D, Cater H L, Banks G and Nolan P M 2018 Assessing mouse behaviour throughout the light/dark cycle using automated in-cage analysis tools. *J. Neurosci. Methods* **300** 37–47

[32] Tsoar A, Nathan R, Bartan Y, Vyssotski A, Dell'Omo G and Ulanovsky N 2011 Large-scale navigational map in a mammal. *Proc Natl Acad Sci USA* **108** E718-24

[33] Kim J, Chung Y, Choi Y, Sa J, Kim H, Chung Y, Park D and Kim H 2017 Depth-Based Detection of Standing-Pigs in Moving Noise Environments. *Sensors Basel Sensors* **17**

[34] Crispim Junior C F, Pederiva C N, Bose R C, Garcia V A, Lino-de-Oliveira C and Marino-Neto J 2012 ETHOWATCHER: validation of a tool for behavioral and video-tracking analysis in laboratory animals. *Comput. Biol. Med.* **42** 257–64

[35] Noldus L P, Spink A J and Tegelenbosch R A 2001 EthoVision: a versatile video tracking system for automation of behavioral experiments. *Behav. Res. Methods Instrum. Comput.* **33** 398–414

[36] Saxena R, Barde W and Deshmukh S S 2018 Inexpensive, scalable camera system for tracking rats in large spaces *BioRxiv*

[37] Miceli S, Nadif Kasri N, Joosten J, Huang C, Kepser L, Proville R, Selten M M, van Eijs F, Azarfar A, Homberg J R, Celikel T and Schubert D 2017 Reduced Inhibition within Layer IV of Sert Knockout Rat Barrel Cortex is Associated with Faster Sensory Integration. *Cereb. Cortex* **27** 933–49

[38] Samson A L, Ju L, Ah Kim H, Zhang S R, Lee J A A, Sturgeon S A, Sobey C G, Jackson S P and Schoenwaelder S M 2015 MouseMove: an open source program for semi-automated analysis of

movement and cognitive testing in rodents. *Sci. Rep.* **5** 16171

[39] Hoogland T M, De Gruijl J R, Witter L, Canto C B and De Zeeuw C I 2015 Role of Synchronous Activation of Cerebellar Purkinje Cell Ensembles in Multi-joint Movement Control. *Curr. Biol.* **25** 1157–65

[40] Machado A S, Darmohray D M, Fayad J, Marques H G and Carey M R 2015 A quantitative framework for whole-body coordination reveals specific deficits in freely walking ataxic mice. *elife* **4**

[41] Nashaat M A, Oraby H, Peña L B, Dominiak S, Larkum M E and Sachdev R N S 2017 Pixying Behavior: A Versatile Real-Time and Post Hoc Automated Optical Tracking Method for Freely Moving and Head Fixed Animals. *Eneuro* **4**

[42] Voigts J, Herman D H and Celikel T 2015 Tactile object localization by anticipatory whisker motion. *J. Neurophysiol.* **113** 620–32

[43] Wallace D J, Greenberg D S, Sawinski J, Rulla S, Notaro G and Kerr J N D 2013 Rats maintain an overhead binocular field at the expense of constant fusion. *Nature* **498** 65–9

[44] Payne H L and Raymond J L 2017 Magnetic eye tracking in mice. *elife* **6**

[45] Mendes C S, Bartos I, Márka Z, Akay T, Márka S and Mann R S 2015 Quantification of gait parameters in freely walking rodents. *BMC Biol.* **13** 50

[46] Hamers F P, Lankhorst A J, van Laar T J, Veldhuis W B and Gispen W H 2001 Automated quantitative gait analysis during overground locomotion in the rat: its application to spinal cord contusion and transection injuries. *J. Neurotrauma* **18** 187–201

[47] Risse B, Thomas S, Otto N, Löpmeier T, Valkov D, Jiang X and Klämbt C 2013 FIM, a novel FTIR-based imaging method for high throughput locomotion analysis. *PLoS ONE* **8** e53963

[48] Mabrouk O S, Dripps I J, Ramani S, Chang C, Han J L, Rice K C and Jutkiewicz E M 2014 Automated touch screen device for recording complex rodent behaviors. *J. Neurosci. Methods* **233** 129–36

[49] Shih Y-H, Ke T-C, Lin M-T and Young M-S 2008 Sensor system for enhanced detection of locomotion and standing behavior in rats *IEEE Sens. J.* **8** 357–64

[50] Han J Y 2005 Low-cost multi-touch sensing through frustrated total internal reflection *Proceedings of the 18th annual ACM symposium on User interface software and technology - UIST '05* the 18th annual ACM symposium (New York, New York, USA: ACM Press) p 115

[51] Novotný M, Lacko J and Samuelčík M 2013 Applications of Multi-touch Augmented Reality System in Education and Presentation of Virtual Heritage *Procedia Computer Science* **25** 231–5

[52] Shimshek D R, Jensen V, Celikel T, Geng Y, Schupp B, Bus T, Mack V, Marx V, Hvalby Ø, Seeburg P H and Sprengel R 2006 Forebrain-specific glutamate receptor B deletion impairs spatial memory but not hippocampal field long-term potentiation. *J. Neurosci.* **26** 8428–40

[53] Hines T J and Minton B R 2012 Effects of Environmental Enrichment on Rat Behavior in the Open Field Test *2012 NCUR*

[54] Willis E F, Bartlett P F and Vukovic J 2017 Protocol for Short- and Longer-term Spatial Learning and Memory in Mice. *Front. Behav. Neurosci.* **11** 197

[55] Cimadevilla J M, Kaminsky Y, Fenton A and Bures J 2000 Passive and active place avoidance as a tool of spatial memory research in rats. *J. Neurosci. Methods* **102** 155–64

[56] Straw A D, Branson K, Neumann T R and Dickinson M H 2010 Multi-camera Realtime 3D Tracking of Multiple Flying Animals *arXiv*

[57] Del Grosso N A, Graboski J J, Chen W, Blanco Hernández E and Sirota A 2017 Virtual Reality system for freely-moving rodents. *BioRxiv*

[58] Dan Y and Poo M-M 2004 Spike timing-dependent plasticity of neural circuits. *Neuron* **44** 23–30

[59] Foeller E, Celikel T and Feldman D E 2005 Inhibitory sharpening of receptive fields contributes to whisker map plasticity in rat somatosensory cortex. *J. Neurophysiol.* **94** 4387–400

[60] Allen C B, Celikel T and Feldman D E 2003 Long-term depression induced by sensory deprivation during cortical map plasticity in vivo. *Nat. Neurosci.* **6** 291–9

[61] Celikel T, Szostak V A and Feldman D E 2004 Modulation of spike timing by sensory deprivation during induction of cortical map plasticity. *Nat. Neurosci.* **7** 534–41

[62] Clem R L, Celikel T and Barth A L 2008 Ongoing in vivo experience triggers synaptic metaplasticity in the neocortex. *Science* **319** 101–4

[63] Juczewski K, von Richthofen H, Bagni C, Celikel T, Fisone G and Krieger P 2016 Somatosensory map expansion and altered processing of tactile inputs in a mouse model of fragile X syndrome. *Neurobiol. Dis.* **96** 201–15

[64] Voigts J, Sakmann B and Celikel T 2008 Unsupervised whisker tracking in unrestrained behaving animals. *J. Neurophysiol.* **100** 504–15

[65] Rolston J D, Gross R E and Potter S M 2010 Closed-loop, open-source electrophysiology. *Front. Neurosci.* **4**

[66] Patel Y A, George A, Dorval A D, White J A, Christini D J and Butera R J 2017 Hard real-time closed-loop electrophysiology with the Real-Time eXperiment Interface (RTXI). *PLoS Comput. Biol.* **13** e1005430

[67] Shi Q, Ishii H, Kinoshita S, Konno S, Takanishi A, Okabayashi S, Iida N and Kimura H 2013 A rat-like robot for interacting with real rats *Robotica* **31** 1337–50

[68] Kim E J, Park M, Kong M-S, Park S G, Cho J and Kim J J 2015 Alterations of hippocampal place cells in foraging rats facing a “predatory” threat. *Curr. Biol.* **25** 1362–7

[69] Wilson J C, Kesler M, Pelegrin S-L E, Kalvi L, Gruber A and Steenland H W 2015 Watching from a distance: A robotically controlled laser and real-time subject tracking software for the study of conditioned predator/prey-like interactions. *J. Neurosci. Methods* **253** 78–89

[70] Gianelli S, Harland B and Fellous J-M 2018 A new rat-compatible robotic framework for spatial navigation behavioral experiments. *J. Neurosci. Methods* **294** 40–50